



Research article

The fractal-fractional Atangana-Baleanu operator for pneumonia disease: stability, statistical and numerical analyses

Najat Almutairi¹, Sayed Saber^{2,3} and Hijaz Ahmad^{4,5,6,*}

¹ Department of Mathematics, College of Science, Qassim University, Buraidah, Saudi Arabia

² Department of Mathematics and Statistics, Faculty of Science, Beni-Suef University, Egypt

³ Department of Mathematics, Faculty of Science and Arts in Baljurashi, Al-Baha University, Saudi Arabia

⁴ Near East University, Operational Research Center in Healthcare, Nicosia, Turkey

⁵ Department of Computer Science and Mathematics, Lebanese American University, Beirut, Lebanon

⁶ Section of Mathematics, International Telematic University Uninettuno, Corso Vittorio Emanuele II, 39, 00186, Rome, Italy

* **Correspondence:** Email: hijaz555@gmail.com; Tel: +923209052093.

Abstract: The present paper studies pneumonia transmission dynamics by using fractal-fractional operators in the Atangana-Baleanu sense. Our model predicts pneumonia transmission dynamically. Our goal is to generalize five ODEs of the first order under the assumption of five unknowns (susceptible, vaccinated, carriers, infected, and recovered). The Atangana-Baleanu operator is used in addition to analysing existence, uniqueness, and non-negativity of solutions, local and global stability, Hyers-Ulam stability, and sensitivity analysis. As long as the basic reproduction number \mathcal{R}_0 is less than one, the free equilibrium point is local, asymptotic, or otherwise global. Our sensitivity statistical analysis shows that \mathcal{R}_0 is most sensitive to pneumonia disease density. Further, we compute a numerical solution for the model by using fractal-fractional. Graphs of the results are presented for demonstration of our proposed method. The results of the Atangana-Baleanu fractal-fractional scheme is in excellent agreement with the actual data.

Keywords: fractional derivatives; nonlinear equations; simulation; numerical results; infectious disease; time varying control system

Mathematics Subject Classification: 34C60, 92B05, 92C42, 92D25, 92D30

1. Introduction

Infections of the lungs, such as pneumonia, have a variety of causes. The prevalence of this disease is increasing in all age groups and is a major medical concern. Several researchers are working on mathematical models that describe disease spread and optimal control problems in epidemics because they are highly interesting. As a result, these models play a critical role in predicting the effects of epidemics and diseases on areas and populations, as well as the environment. Researchers have presented models for modeling pneumonia dynamics based on a review of the literature; see, e.g., [1–8]. Based on a mathematical analysis of pneumonia and typhoid characteristics, Tilahun et al. [6] proposed a coinfection model. Tilahun et al. [7] used ordinary differential equations and a few theorems to model pneumonia and meningitis coinfections in 2018.

Since 1970, infectious disease dynamics has emerged as an interdisciplinary field. Epidemiology studies disease spread. Modeling diseases and their effects on humans is described in [5]. Fractional and fractal calculus are combined here. In engineering, physics, biology, and biomedicine, fractal-fractional operators are widely used to model real-world processes. Comparable to classical models, fractional order integrals and fractional derivatives are more precise than classical models. In fractional derivatives, there are three different types of operators: Riemann-Liouville and Caputo, Caputo-Fabrizio and Atangana-Baleanu, which are connected to power laws, exponential decay laws, and extended Mittag-Leffler functions [9–52].

The concept of fractal-fractional order integration and differentiation was developed by Atangana with two orders, i.e., one fractional and the other fractal [53, 54]. Besides, fractal differentiation is equivalent to classical differentiation if the fractal order tends to 1. Fractal behaviors are investigated through the use of these combined operators. Several researchers have shown that fractal-fractional operators better capture real-world mathematics [55–79]. These include but are not limited to, for instance, the HIV/AIDS model [57], Leishmania model [58], tuberculosis model [59], Q fever model [60], hepatitis C virus model [61], AH1N1/09 virus model [62] and tobacco smoking model [63].

This study investigates the formulation of the Tilahun et al. mathematical model of pneumonia transmission dynamics by using fractal-fractional derivatives in the Atangana-Baleanu sense. The model is improved by assuming five unknowns and using this Caputo, and Atangana-Baleanu-type fractional derivatives. The study aims to investigate and compare the solutions to this system, which unique as compared to other studies. The authors construct schemes for this system, using the fractal-fractional Atangana-Baleanu operator to prove the existence, uniqueness, non-negativity and boundedness of solutions. Three levels of stability are established: local, global and Hyers-Ulam. Sensitivity analysis is conducted to assess the impact of parameters on initial disease transmission. The study finds that \mathcal{R}_0 is most sensitive to pneumonia disease density. The results show that the scheme's method is effective and suitable for the system defined by Caputo and Atangana-Baleanu fractional derivatives. Simulations using Matlab show that the schemes method is suitable for both types of problems and has approximate solutions that are close to the exact solution. The study also discusses other fractional operators and numerically verifies their mathematical findings for the proposed model's dynamical behavior.

2. Preliminaries

2.1. Fractal-fractional pneumonia model

Definition 1 ([76, 77]). Consider the fractal to be differentiable on (a, b) of order $0 < \tau_2 \leq 1$ for $\phi \in C((a, b), \mathbb{R})$. The following is a fractal-fractional derivative operator for t in the Atangana-Baleanu setting:

$${}^{FF-AB} \mathcal{D}_{0,t}^{\tau_1, \tau_2} \phi(t) = \frac{\hbar(\tau_1)}{1 - \tau_1} \frac{d}{dt^{\tau_2}} \int_0^t \phi(s) E_{\tau_1} \left[-\frac{\tau_1}{1 - \tau_1} (t - s)^{\tau_1} \right] ds,$$

where, $\hbar(\tau_1) = 1 - \tau_1 + \frac{\tau_1}{\Gamma(\tau_1)}$, and $\frac{dh(s)}{ds^{\tau_2}} = \lim_{t \rightarrow s} \frac{h(t) - h(s)}{t^{\tau_2} - s^{\tau_2}}$.

Definition 2 ([76, 77]). The fractal-fractional integration operator is given by

$${}^{FF-AB} I_{0,t}^{\tau_1, \tau_2} \phi(t) = \frac{\tau_1 \tau_2}{\hbar(\tau_1) \Gamma(\tau_1)} \int_0^t s^{\tau_2 - 1} \phi(s) (t - s)^{\tau_1 - 1} ds + \frac{\tau_2 (1 - \tau_1) t^{\tau_2 - 1}}{\hbar(\tau_1)} \phi(t).$$

There are five populations in the pneumonia model: susceptible (x), vaccinated (y), carrier (z), infected (u) and recovered (v). The total human population, denoted by N , can be expressed as $N = x + y + z + u + v$. Therefore, our suggested fractal-fractional pneumonia model in the sense of the Atangana-Baleanu derivative looks like this:

$$\begin{aligned} {}^{FF-AB} \mathcal{D}_{0,t}^{\tau_1, \tau_2} x(t) &= (1 - p)\pi + \phi y(t) + \delta v(t) - (\vartheta + \mu + \lambda) x(t), \\ {}^{FF-AB} \mathcal{D}_{0,t}^{\tau_1, \tau_2} y(t) &= p\pi + \vartheta x(t) - (\phi + \mu + \varepsilon\lambda) y(t), \\ {}^{FF-AB} \mathcal{D}_{0,t}^{\tau_1, \tau_2} z(t) &= \varrho\lambda x(t) + \varrho\varepsilon\lambda y(t) + \eta(1 - q) u(t) - (\beta + \chi + \mu) z(t), \\ {}^{FF-AB} \mathcal{D}_{0,t}^{\tau_1, \tau_2} u(t) &= \lambda(1 - \varrho) x(t) + \varepsilon\lambda(1 - \varrho) y(t) + \chi z(t) - (\alpha + \eta + \mu) u(t), \\ {}^{FF-AB} \mathcal{D}_{0,t}^{\tau_1, \tau_2} v(t) &= \beta z(t) + q\eta u(t) - (\delta + \mu) v(t), \end{aligned} \tag{2.1}$$

subject to $x(0) \geq 0, y(0) \geq 0, z(0) \geq 0, u(0) \geq 0, v(0) \geq 0$.

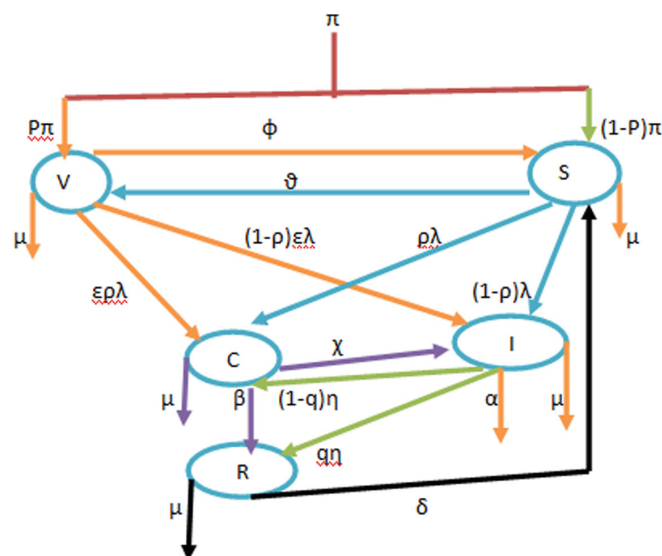


Figure 1. Model flow diagram for (2.1) with $x(t) = S(t), y(t) = V(t), z(t) = C(t), u(t) = I(t), v(t) = R(t)$ [6].

All of the positive parameters are listed in Table 1. When people get infected, they either join the carrier class z or the infectious class u based on a probability of $1 - \varrho$. Let Υ be the transmission coefficient for the carrier. Infection force is defined as $\lambda = az + bu$, where $a = \frac{k\tau\Upsilon}{N}$ represents the carrier compartment transmission and $b = \frac{k\tau}{N}$ represents the infective compartment transmission. The population is $N = x(t) + y(t) + z(t) + u(t) + v(t)$. If $\Upsilon > 1$, carriers are more likely to infect susceptibles than infectious individuals. Both carriers and infectives have the same chance of spreading when $\Upsilon = 1$. Nevertheless, if $\Upsilon < 1$, the infective has a higher chance of contacting the susceptible.

Table 1. The values of the applied parameters.

Parameters symbols	Description	Source	Values
k	The contact rate	Estimated	0.5
ϵ	The transmission coefficient for the carrier	[2]	0.002
τ	The probability that a contact causes infection	[2]	0.89 – 0.99
ϕ	The rate of the susceptible class increased from the vaccinated class	[6]	0.0025
ψ	The proportion of the serotype not covered by the vaccine	Assumed	0.2
δ	The rate at which individuals in the recovery class lose their temporary immunity	[2]	0.1
χ	The rate of infection	[2]	0.001 – 0.01096
p	The rate at which a fraction of the population was vaccinated before the disease outbreak	[2]	0.2
θ	The rate of population movement from the susceptible class to the vaccinated class	Assumed	0.008
μ	The natural death rate of the population in all compartments	Estimated	0.01
α	The rate of dying from the disease	Estimated	0.0057
Θ	$\Theta = k\tau$	[6]	0.05
β	Recovery rate after gaining immunity	[6]	0.0115
η	Treatment rate per capita in the infected class moving to the recovered compartment	[6]	0.2
q	Treatment efficacy	[6]	0.5 – 1
Υ	The infection force	Assumed	1.2

2.2. Existence and uniqueness

The matrix form of (1.2) is given by:

$$\begin{aligned} {}^{\text{FF-AB}}\mathcal{D}_{0,t}^{\tau_1, \tau_2} \Psi(t) &= \Lambda(t, \Psi(t)) \\ &= (\Upsilon_1(t, \Psi(t)), \Upsilon_2(t, \Psi(t)), \Upsilon_3(t, \Psi(t)), \Upsilon_4(t, \Psi(t)), \Upsilon_5(t, \Psi(t))), \\ \Psi(t) &= (x(t), y(t), z(t), u(t), v(t)), \quad \Psi(0) = (x(0), y(0), z(0), u(0), v(0)). \end{aligned} \quad (2.2)$$

Define the Banach space $\mathbb{U} = X^5$, where $X = C(I, \mathbb{R})$ is subject to the norm

$$\|\mathcal{H}\| = \max_{t \in [0,1]} |x(t) + y(t) + z(t) + u(t) + v(t)|.$$

$$\mathcal{H}(\Psi)(t) = \Psi(0) + \frac{\tau_2 t^{\tau_2-1}(1-\tau_1)}{AB(\tau_1)} \Lambda(t, \Psi(t)) + \frac{\tau_1 \tau_2}{AB(\tau_1)\Gamma(\tau_1)} \int_0^t \xi^{\tau_2-1} (t-\xi)^{\tau_2-1} \Lambda(\xi, \Psi(\xi)) d\xi. \quad (2.3)$$

Let $\|x\| \leq \eta_1$, $\|y\| \leq \eta_2$, $\|z\| \leq \eta_3$, $\|u\| \leq \eta_4$ and $\|v\| \leq \eta_5$ for some constants $\eta_1, \eta_2, \eta_3, \eta_4, \eta_5 > 0$.

Rewrite (2.1) as follows

$$\begin{aligned} {}^{FF-AB}\mathcal{D}_{0,t}^{\tau_1, \tau_2} x(t) &= \tau_2 t^{\tau_2-1} \Upsilon_1(t, \Psi(t)), \\ {}^{FF-AB}\mathcal{D}_{0,t}^{\tau_1, \tau_2} y(t) &= \tau_2 t^{\tau_2-1} \Upsilon_2(t, \Psi(t)), \\ {}^{FF-AB}\mathcal{D}_{0,t}^{\tau_1, \tau_2} z(t) &= \tau_2 t^{\tau_2-1} \Upsilon_3(t, \Psi(t)), \\ {}^{FF-AB}\mathcal{D}_{0,t}^{\tau_1, \tau_2} u(t) &= \tau_2 t^{\tau_2-1} \Upsilon_4(t, \Psi(t)), \\ {}^{FF-AB}\mathcal{D}_{0,t}^{\tau_1, \tau_2} v(t) &= \tau_2 t^{\tau_2-1} \Upsilon_5(t, \Psi(t)), \end{aligned}$$

where

$$\begin{aligned} \Upsilon_1(t, \Psi(t)) &= (1-p)\pi + \phi y(t) + \delta v(t) - (\vartheta + \mu + \lambda) x(t), \\ \Upsilon_2(t, \Psi(t)) &= p\pi + \vartheta x(t) - (\mu + \lambda\epsilon + \phi) y(t), \\ \Upsilon_3(t, \Psi(t)) &= \varrho\lambda x(t) + \varrho\epsilon\lambda y(t) + \eta(1-q)u(t) - (\beta + \chi + \mu) z(t), \\ \Upsilon_4(t, \Psi(t)) &= \lambda(1-\varrho)x(t) + \epsilon\lambda(1-\varrho)y(t) + \chi z(t) - (\alpha + \eta + \mu) u(t), \\ \Upsilon_5(t, \Psi(t)) &= \beta z(t) + q\eta u(t) - (\delta + \mu) v(t). \end{aligned}$$

Applying fractional integrals, we get

$$\Psi(t) = \Psi(0) + \frac{\tau_2 t^{\tau_2-1}(1-\tau_1)}{\hbar(\tau_1)} \Lambda(t, \Psi(t)) + \frac{\tau_1 \tau_2}{\hbar(\tau_1)\Gamma(\tau_1)} \int_0^t \xi^{\tau_2-1} (t-\xi)^{\tau_2-1} \Lambda(\xi, \Psi(\xi)) d\xi.$$

$\Lambda(t, \Psi(t))$ must satisfy these Lipschitz and growth conditions.

Theorem 1. For each $\Psi_1, \Psi_2 \in \mathcal{B}$, \exists a constant $A > 0$ that satisfies

$$|\Lambda(t, \Psi_1(t)) - \Lambda(t, \Psi_2(t))| \leq A |\Psi_1(t) - \Psi_2(t)|, \quad (2.4)$$

where $A = \max\{\omega_1, \omega_2, \omega_3, \omega_4, \omega_5\}$, with $\omega_1 = \mu + 2\lambda + 2\lambda\varrho + 2\vartheta$, $\omega_2 = \mu + 2\phi + 2\epsilon\lambda + 2\lambda\epsilon\varrho$, $\omega_3 = 2\chi + \mu + 2\beta$, $\omega_4 = 2q\eta + \mu + \alpha + 2\eta$, $\omega_5 = 2\delta + \mu$.

Proof. For each $\Psi_1, \Psi_2 \in \mathcal{B}$, one obtains

$$\begin{aligned} \|\Lambda(t, \Psi_1(t)) - \Lambda(t, \Psi_2(t))\| &\leq \omega_1 |x_1 - x_2| + \omega_2 |y_1 - y_2| \\ &\quad + \omega_3 |z_1 - z_2| + \omega_4 |u_1 - u_2| + \omega_5 |v_1 - v_2| \\ &\leq A |\Psi_1(t) - \Psi_2(t)|. \end{aligned}$$

Therefore, $\Lambda(t, \Psi(t))$ satisfies the Lipschitz condition. \square

Theorem 2. There are constants $\mathbf{z}_\Psi > 0$ and \mathbb{M}_Ψ satisfies the following, for each Ψ in \mathcal{B} ,

$$|\Lambda(t, \Psi(t))| \leq \mathbf{z}_\Psi |\Psi(t)| + \mathbb{M}_\Psi.$$

So, there is at least one solution to the suggested model.

Proof. To begin with, we demonstrate that the operator Λ stated in (2.2) is totally continuous. Due to the continuous nature of Ψ , N is also continuous. \square

Theorem 3. Assume that (2.4) is true; then,

$$\Xi = \left(\frac{\tau_2 T^{\tau_2-1}(1-\tau_1)}{\hbar(\tau_1)} + \frac{\tau_1 \tau_2}{\hbar(\tau_1) \Gamma(\tau_1)} T^{\mu+\tau_2-1} \mathbf{H}(\xi, \tau_2) \right) A.$$

So, it has a unique solution.

Proof. For Ψ_1, Ψ_2 in \mathcal{B} , we obtain

$$\begin{aligned} |\mathcal{H}(\Psi_1) - \mathcal{H}(\Psi_2)| &= \max_{t \in [0, T]} \left| \frac{\tau_2 t^{\tau_2-1}(1-\tau_1)}{\hbar(\tau_1)} (\Lambda(t, \Psi_1(t)) - \Lambda(t, \Psi_2(t))) \right. \\ &\quad \left. + \frac{\tau_1 \tau_2}{\hbar(\tau_1) \Gamma(\tau_1)} \int_0^t \xi^{\tau_2-1} (t-\xi)^{\tau_2-1} (\Lambda(\xi, \Psi_1(\xi)) - \Lambda(\xi, \Psi_2(\xi))) d\xi \right| \\ &\leq A \left[\frac{\tau_2 t^{\tau_2-1}(1-\tau_1)}{\hbar(\tau_1)} + \frac{\tau_1 \tau_2}{\hbar(\tau_1) \Gamma(\tau_1)} T^{\mu+\tau_2-1} \mathbf{H}(\xi, \tau_2) \right] \|\Psi_1 - \Psi_2\| \\ &\leq \Xi \|\Psi_1 - \Psi_2\|. \end{aligned}$$

Due to this, \mathcal{H} is a contraction and there is only one solution to the model. \square

The non-negativity and boundedness of the solutions of the system (2.1) in the fractional case have been proved in [8].

3. Model analysis

An infection-free equilibrium is $E^0 = (x_0, y_0, 0, 0, 0) = \left(\frac{\pi \mathfrak{N}_1}{\mu}, \frac{\pi \mathfrak{N}_2}{\mu}, 0, 0, 0 \right)$, with $\mathfrak{N}_1 = \frac{\mu + \phi - \rho \mu}{\mu + \phi + \vartheta}$ and $\mathfrak{N}_2 = \frac{\vartheta + \rho \mu}{\mu + \phi + \vartheta}$ for $z = u = v = 0$. The endemic equilibrium, given as $E^* = (x^*, y^*, z^*, u^*, v^*)$ for $u > 0, z > 0$ was acquired by applying the following:

$$\begin{cases} {}^{\text{FF-AB}} \mathcal{D}_{0,t}^{\tau_1, \tau_2} x(t) = 0, \\ {}^{\text{FF-AB}} \mathcal{D}_{0,t}^{\tau_1, \tau_2} y(t) = 0, \\ {}^{\text{FF-AB}} \mathcal{D}_{0,t}^{\tau_1, \tau_2} z(t) = 0, \\ {}^{\text{FF-AB}} \mathcal{D}_{0,t}^{\tau_1, \tau_2} u(t) = 0, \\ {}^{\text{FF-AB}} \mathcal{D}_{0,t}^{\tau_1, \tau_2} v(t) = 0. \end{cases}$$

Thus, $E^* = (x^*, y^*, z^*, u^*, v^*) = (E_5 + E_6 u^*, E_3 + E_4 E_5 + E_4 E_6 u^*, E_1 u^*, u^*, E_2 u^*)$, with

$$\begin{aligned} E_1 &= \frac{(1-\varrho)\eta(1-q) + \varrho\Phi}{(1-\varrho)(\beta + \chi + \mu) + \varrho\chi}, & E_2 &= \frac{\beta E_1 + q\eta}{\delta + \mu}, & E_3 &= \frac{\rho\pi}{\phi + \mu + \varepsilon\lambda}, \\ E_4 &= \frac{\theta}{\phi + \mu + \varepsilon\lambda}, & E_5 &= \frac{(1-p)\pi + \phi E_3}{\mu + \lambda + \theta - \phi E_4}, & E_6 &= \frac{\delta E_2}{\mu + \lambda + \theta - \phi E_4}, \\ u^* &= \frac{\rho\pi + \theta E_5 - (\phi + \mu + \varepsilon\lambda)(E_3 + E_4 E_5)}{-\Psi E_6 + (\mu + \varepsilon\lambda + (\alpha + \eta + \mu)) E_4 E_6}. \end{aligned}$$

The basic reproduction number is given by [7, 8],

$$\mathcal{R}_0 = \frac{[\varrho b\chi + a\varrho(\alpha + \eta + \mu) + a\eta(1 - \varrho)(1 - q) + b(\beta + \chi + \mu)(1 - \varrho)]}{(\beta + \chi + \mu)(\alpha + \eta + \mu) - \eta(1 - q)\chi} (x_0 + \epsilon y_0).$$

3.1. Stability of an infection-free equilibrium E_0

Lemma 1. *If $\mathcal{R}_0 = 1$, E_0 is locally asymptotically stable for model (2.1), and unstable if $\mathcal{R}_0 > 1$. Moreover, model (2.1) has a globally asymptotically stable E_0 .*

Proof. The first part follows as in [8]. We present a positive definite Lyapunov function:

$$L_1 = \left(x - x_0 - x_0 \ln \frac{x}{x_0} \right) + \left(y - y_0 - y_0 \ln \frac{y}{y_0} \right).$$

One obtains

$$\begin{aligned} {}^{\text{FF-AB}}\mathcal{D}_{0,t}^{\tau_1, \tau_2} L_1 &\leq \left(\frac{x - x_0}{x} \right) {}^{\text{FF-AB}}\mathcal{D}_{0,t}^{\tau_1, \tau_2} x + \left(\frac{y - y_0}{y} \right) {}^{\text{FF-AB}}\mathcal{D}_{0,t}^{\tau_1, \tau_2} y \\ &= \left(\frac{x - x_0}{x} \right) \left((1 - p)\pi + \phi y(t) + \delta v(t) - (\vartheta + \mu + \lambda) x(t) \right) \\ &\quad + \left(\frac{y - y_0}{y} \right) \left(p\pi + \vartheta x(t) - (\phi + \mu + \epsilon\lambda) y(t) \right). \end{aligned}$$

At E_0 , one obtains

$$\begin{aligned} {}^{\text{FF-AB}}\mathcal{D}_{0,t}^{\tau_1, \tau_2} L_1 &\leq \left(\frac{x - x_0}{x} \right) {}^{\text{FF-AB}}\mathcal{D}_{0,t}^{\tau_1, \tau_2} x + \left(\frac{y - y_0}{y} \right) {}^{\text{FF-AB}}\mathcal{D}_{0,t}^{\tau_1, \tau_2} y \\ &= (x - x_0) \left(\frac{(1 - p)\pi}{x} + \frac{\phi y}{x} + \frac{\delta v}{x} - (\vartheta + \mu + \lambda) \right) \\ &\quad + (y - y_0) \left(\frac{p\pi}{y} + \frac{\vartheta x}{y} - (\phi + \mu + \epsilon\lambda) \right) \\ &= -\frac{(1 - p)\pi}{x x_0} (x - x_0)^2 - \frac{(\alpha + \eta + \mu)V}{x x_0} (x - x_0)^2 \\ &\quad - \frac{\delta v}{x x_0} (x - x_0)^2 - \frac{p\pi}{y y_0} (y - y_0)^2 - \frac{\vartheta x}{y y_0} (y - y_0)^2. \end{aligned}$$

Thus, ${}^{\text{FF-AB}}\mathcal{D}_{0,t}^{\tau_1, \tau_2} L_1 < 0$ for all $(x, y, z, u, v) \in \Lambda$. Moreover, ${}^{\text{FF-AB}}\mathcal{D}_{0,t}^{\tau_1, \tau_2} L_1 = 0$ implies that $x = x_0$, $y = y_0$, $z = z_0$, $u = u_0$ and $v = v_0$. So, $\{E_0\}$ is the only set satisfying that ${}^{\text{FF-AB}}\mathcal{D}_{0,t}^{\tau_1, \tau_2} L_1 = 0$. \square

3.2. Stability of an endemic equilibrium E^*

Lemma 2. *E^* exists when $\mathcal{R}_0 > 1$; otherwise, there is no endemic equilibrium.*

Proof. The following characteristics are required for a disease to be endemic: ${}^{\text{FF-AB}}\mathcal{D}_{0,t}^{\tau_1, \tau_2} z(t) > 0$ and ${}^{\text{FF-AB}}\mathcal{D}_{0,t}^{\tau_1, \tau_2} u(t) > 0$, that is,

$$\begin{aligned} {}^{\text{FF-AB}}\mathcal{D}_{0,t}^{\tau_1, \tau_2} z(t) &= \varrho\lambda x(t) + \varrho\epsilon\lambda y(t) + \eta(1 - q)u(t) - (\beta + \chi + \mu)z(t) > 0, \\ {}^{\text{FF-AB}}\mathcal{D}_{0,t}^{\tau_1, \tau_2} u(t) &= \lambda(1 - \varrho)x(t) + \epsilon\lambda(1 - \varrho)y(t) + \chi z(t) - (\alpha + \eta + \mu)u(t) > 0. \end{aligned} \quad (3.1)$$

Given (3.1), based on the first inequality,

$$(\beta + \chi + \mu) z(t) < \varrho \lambda x(t) + \varrho \varepsilon \lambda y(t) + \eta(1 - q) u(t).$$

Then,

$$z(t) < \frac{\varrho \alpha \left(\frac{u(t) + \gamma y(t)}{N} \right) (x(t) + \varepsilon y(t)) + \eta(1 - q) u(t)}{(\beta + \chi + \mu)}.$$

Because $\frac{(x(t) + \varepsilon y(t))}{N} \leq 1$, one obtains

$$z(t) < \frac{\varrho \alpha u(t) + \eta(1 - q) u(t)}{(\beta + \chi + \mu) - \varrho \alpha \gamma}. \quad (3.2)$$

As a result of the second inequality of (3.1),

$$(\alpha + \eta + \mu) u(t) < \lambda(1 - \varrho) x(t) + \varepsilon \lambda(1 - \varrho) y(t) + \chi y(t).$$

Then,

$$u(t) < \frac{(1 - \varrho) \alpha \left(\frac{u(t) + \gamma y(t)}{N} \right) (x(t) + \varepsilon y(t)) + \chi y(t)}{(\alpha + \eta + \mu)}.$$

Using the fact that $\frac{(x(t) + \varepsilon y(t))}{N} \leq 1$, one obtains

$$u(t) < \frac{(1 - \varrho) \alpha u(t) + (1 - \varrho) \alpha \gamma y(t) + \chi y(t)}{(\alpha + \eta + \mu)}. \quad (3.3)$$

Substituting (3.2) into (3.3), one obtains

$$u(t) < \frac{(1 - \varrho) \alpha u((\beta + \chi + \mu) - \varrho \alpha \gamma) + (1 - \varrho) \alpha \gamma (\varrho \alpha u + \eta(1 - q) u) + \chi (\varrho \alpha u + \eta(1 - q) u)}{(\beta + \chi + \mu - \varrho \alpha \gamma)(\alpha + \eta + \mu)}.$$

After rearranging and canceling $u(t)$, one gets

$$\begin{aligned} 1 &< \alpha \left[\frac{(1 - \varrho)(\gamma \eta(1 - q) + (\beta + \chi + \mu))}{(\alpha + \eta + \mu)(\beta + \chi + \mu) - \chi \eta(1 - q)} + \frac{\varrho(\gamma(\alpha + \eta + \mu) + \chi)}{(\alpha + \eta + \mu)(\beta + \chi + \mu) - \chi \eta(1 - q)} \right] \\ &\leq \alpha \left[\frac{(1 - \varrho)(\gamma \eta(1 - q) + (\beta + \chi + \mu))}{(\beta + \chi + \mu)(\alpha + \eta + \mu) - \eta(1 - q)\chi} + \frac{\varrho(\gamma(\alpha + \eta + \mu) + \chi)}{(\beta + \chi + \mu)(\alpha + \eta + \mu) - \eta(1 - q)\chi} \right] \left(\frac{\pi \mathfrak{R}_1}{\mu} + \frac{\pi \mathfrak{R}_2}{\mu} \right) \\ &= \mathfrak{R}_0. \end{aligned}$$

Thus, $\mathfrak{R}_0 > 1$ creates a unique endemic equilibrium. \square

Lemma 3 ([8]). E^* is locally asymptotically stable for $\mathfrak{R}_0 > 1$. Moreover, E^* is globally asymptotically stable.

Proof. Define

$$\begin{aligned} L_2 &= \left(x - x^* - x^* \ln \frac{x}{x^*} \right) + \left(y - y^* - y^* \ln \frac{y}{y^*} \right) + \left(z - z^* - z^* \ln \frac{z}{z^*} \right) \\ &\quad + \left(u - u^* - u^* \ln \frac{u}{u^*} \right) + \left(v - v^* - v^* \ln \frac{v}{v^*} \right). \end{aligned}$$

Thus, one obtains

$$\begin{aligned} {}^{\text{FF-AB}}\mathcal{D}_{0,t}^{\tau_1,\tau_2} L_2 &\leq \left(\frac{x-x^*}{x}\right) {}^{\text{FF-AB}}\mathcal{D}_{0,t}^{\tau_1,\tau_2} x + \left(\frac{y-y^*}{y}\right) {}^{\text{FF-AB}}\mathcal{D}_{0,t}^{\tau_1,\tau_2} y + \left(\frac{z-z^*}{z}\right) {}^{\text{FF-AB}}\mathcal{D}_{0,t}^{\tau_1,\tau_2} z \\ &+ \left(\frac{u-u^*}{u}\right) {}^{\text{FF-AB}}\mathcal{D}_{0,t}^{\tau_1,\tau_2} u + \left(\frac{v-v^*}{v}\right) {}^{\text{FF-AB}}\mathcal{D}_{0,t}^{\tau_1,\tau_2} v \\ &= -\left(x-x^*\right)^2 \frac{(1-p)\pi}{xx^*} - \left(x-x^*\right)^2 \frac{(\alpha+\eta+\mu)y}{xx^*} - \left(x-x^*\right)^2 \frac{\delta v}{xx^*} - \left(y-y^*\right)^2 \frac{p\pi}{yy^*} \\ &- \left(y-y^*\right)^2 \frac{\vartheta x}{yy^*} - \left(z-z^*\right)^2 \frac{\varrho\lambda x}{zz^*} - \left(z-z^*\right)^2 \frac{\varrho\varepsilon\lambda y}{zz^*} - \left(z-z^*\right)^2 \frac{\eta(1-q)u}{zz^*} - \left(u-u^*\right)^2 \\ &\times \frac{\lambda(1-\varrho)x}{uu^*} - \left(u-u^*\right)^2 \frac{\varepsilon\lambda(1-\varrho)y}{uu^*} - \left(u-u^*\right)^2 \frac{\chi z}{uu^*} - \left(v-v^*\right)^2 \frac{\beta z}{vv^*} - \left(v-v^*\right)^2 \frac{q\eta u}{vv^*}. \end{aligned}$$

Thus, ${}^{\text{FF-AB}}\mathcal{D}_{0,t}^{\tau_1,\tau_2} L_2 < 0$ for all $(x, y, z, u, v) \in \Lambda$. Furthermore, ${}^{\text{FF-AB}}\mathcal{D}_{0,t}^{\tau_1,\tau_2} L_2 = 0$ implies that $x = x^*$, $y = y^*$, $z = z^*$, $u = u^*$, and $v = v^*$. Therefore, according to Theorem 5, E^* is globally asymptotically stable. \square

3.3. Hyers-Ulam stability

The Hyers-Ulam stability has been motivated by the work done in [80, 81].

Definition 3. The constants $\zeta_i > 0$, for $i \in \mathbb{N}_1^5$ must meet the following conditions for every $\zeta_i > 0$, $i \in \mathbb{N}_1^5$, for model (2.1) to have Hyers-Ulam stability:

$$\begin{aligned} \left| x(t) - \frac{\tau_2(1-\tau_1)t^{\tau_2-1}}{\hbar(\tau_1)} \Upsilon_1(t, \Psi(t)) - \frac{\tau_1\tau_2}{\hbar(\tau_1)\Gamma(\tau_1)} \int_0^t \xi^{\tau_2-1} (t-\xi)^{\tau_1-1} \Upsilon_1(\xi, \Psi(\xi)) d\xi \right| &\leq \zeta_1, \\ \left| y(t) - \frac{\tau_2(1-\tau_1)t^{\tau_2-1}}{\hbar(\tau_1)} \Upsilon_2(t, \Psi(t)) - \frac{\tau_1\tau_2}{\hbar(\tau_1)\Gamma(\tau_1)} \int_0^t \xi^{\tau_2-1} (t-\xi)^{\tau_1-1} \Upsilon_2(\xi, \Psi(\xi)) d\xi \right| &\leq \zeta_2, \\ \left| z(t) - \frac{\tau_2(1-\tau_1)t^{\tau_2-1}}{\hbar(\tau_1)} \Upsilon_3(t, \Psi(t)) - \frac{\tau_1\tau_2}{\hbar(\tau_1)\Gamma(\tau_1)} \int_0^t \xi^{\tau_2-1} (t-\xi)^{\tau_1-1} \Upsilon_3(\xi, \Psi(\xi)) d\xi \right| &\leq \zeta_3, \\ \left| u(t) - \frac{\tau_2(1-\tau_1)t^{\tau_2-1}}{\hbar(\tau_1)} \Upsilon_4(t, \Psi(t)) - \frac{\tau_1\tau_2}{\hbar(\tau_1)\Gamma(\tau_1)} \int_0^t \xi^{\tau_2-1} (t-\xi)^{\tau_1-1} \Upsilon_4(\xi, \Psi(\xi)) d\xi \right| &\leq \zeta_4, \\ \left| v(t) - \frac{\tau_2(1-\tau_1)t^{\tau_2-1}}{\hbar(\tau_1)} \Upsilon_5(t, \Psi(t)) - \frac{\tau_1\tau_2}{\hbar(\tau_1)\Gamma(\tau_1)} \int_0^t \xi^{\tau_2-1} (t-\xi)^{\tau_1-1} \Upsilon_5(\xi, \Psi(\xi)) d\xi \right| &\leq \zeta_5. \end{aligned}$$

In the model (2.1), an approximation is $(x_1(t), y_1(t), z_1(t), u_1(t), v_1(t))$, which satisfies the following:

$$\begin{aligned} x_1(t) &= \frac{\tau_2(1-\tau_1)t^{\tau_2-1}}{\hbar(\tau_1)} \Upsilon_1(t, x_1(t)) + \frac{\tau_1\tau_2}{\hbar(\tau_1)\Gamma(\tau_1)} \int_0^t \xi^{\tau_2-1} (t-\xi)^{\tau_1-1} \Upsilon_1(\xi, x_1(\xi)) d\xi, \\ y_1(t) &= \frac{\tau_2(1-\tau_1)t^{\tau_2-1}}{\hbar(\tau_1)} \Upsilon_2(t, y_1(t)) + \frac{\tau_1\tau_2}{\hbar(\tau_1)\Gamma(\tau_1)} \int_0^t \xi^{\tau_2-1} (t-\xi)^{\tau_1-1} \Upsilon_2(\xi, y_1(\xi)) d\xi, \\ z_1(t) &= \frac{\tau_2(1-\tau_1)t^{\tau_2-1}}{\hbar(\tau_1)} \Upsilon_3(t, z_1(t)) + \frac{\tau_1\tau_2}{\hbar(\tau_1)\Gamma(\tau_1)} \int_0^t \xi^{\tau_2-1} (t-\xi)^{\tau_1-1} \Upsilon_3(\xi, z_1(\xi)) d\xi, \end{aligned}$$

$$u_1(t) = \frac{\tau_2(1-\tau_1)t^{\tau_2-1}}{\hbar(\tau_1)} \Upsilon_4(t, u_1(t)) + \frac{\tau_1\tau_2}{\hbar(\tau_1)\Gamma(\tau_1)} \int_0^t \xi^{\tau_2-1}(t-\xi)^{\tau_1-1} \Upsilon_4(\xi, u_1(\xi)) d\xi,$$

$$v_1(t) = \frac{\tau_2(1-\tau_1)t^{\tau_2-1}}{\hbar(\tau_1)} \Upsilon_5(t, v_1(t)) + \frac{\tau_1\tau_2}{\hbar(\tau_1)\Gamma(\tau_1)} \int_0^t \xi^{\tau_2-1}(t-\xi)^{\tau_1-1} \Upsilon_5(\xi, v_1(\xi)) d\xi,$$

so that

$$\begin{aligned} |x - x_1| &\leq v_1 \omega_1, \\ |y - y_1| &\leq v_2 \omega_2, \\ |z - z_1| &\leq v_3 \omega_3, \\ |u - u_1| &\leq v_4 \omega_4, \\ |v - v_1| &\leq v_5 \omega_5. \end{aligned} \tag{3.4}$$

Theorem 4. *If (3.1) is true, then model (2.1) has Hyers-Ulam stability.*

Proof.

$$\begin{aligned} |x - x_1| &= \left| \frac{\tau_2(1-\tau_1)t^{\tau_2-1}}{\hbar(\tau_1)} (\Upsilon_1(t, x(t)) - \Upsilon_1(t, x_1(t))) \right. \\ &\quad \left. + \frac{\tau_1\tau_2}{\hbar(\tau_1)\Gamma(\tau_1)} \int_0^t \xi^{\tau_2-1}(t-\xi)^{\tau_1-1} (\Upsilon_1(\xi, x(\xi)) - \Upsilon_1(\xi, x_1(\xi))) d\xi \right| \\ &\leq \frac{\tau_2(1-\tau_1)t^{\tau_2-1}}{\hbar(\tau_1)} \omega_1 \|x - x_1\| + \frac{\tau_1\tau_2}{\hbar(\tau_1)\Gamma(\tau_1)} \int_0^t \xi^{\tau_2-1}(t-\xi)^{\tau_1-1} \omega_1 \|x - x_1\| d\xi \\ &\leq \left(\frac{\tau_2(1-\tau_1)}{\hbar(\tau_1)} + \frac{\tau_1\tau_2\Gamma(\tau_2)}{\hbar(\tau_1)\Gamma(\tau_1 + \tau_2)} \right) \omega_1 \|x - x_1\|. \end{aligned}$$

Then,

$$|x - x_1| \leq v_1 \omega_1, \text{ with } v_1 = \left(\frac{\tau_2(1-\tau_1)}{\hbar(\tau_1)} + \frac{\tau_1\tau_2\Gamma(\tau_2)}{\hbar(\tau_1)\Gamma(\tau_1 + \tau_2)} \right) \|x - x_1\|.$$

Similarly, one obtains

$$\begin{aligned} |y - y_1| &\leq v_2 \omega_2, \text{ with } v_2 = \left(\frac{\tau_2(1-\tau_1)}{\hbar(\tau_1)} + \frac{\tau_1\tau_2\Gamma(\tau_2)}{\hbar(\tau_1)\Gamma(\tau_1 + \tau_2)} \right) \|y - y_1\|, \\ |z - z_1| &\leq v_3 \omega_3, \text{ with } v_3 = \left(\frac{\tau_2(1-\tau_1)}{\hbar(\tau_1)} + \frac{\tau_1\tau_2\Gamma(\tau_2)}{\hbar(\tau_1)\Gamma(\tau_1 + \tau_2)} \right) \|z - z_1\|, \\ |u - u_1| &\leq v_4 \omega_4, \text{ with } v_4 = \left(\frac{\tau_2(1-\tau_1)}{\hbar(\tau_1)} + \frac{\tau_1\tau_2\Gamma(\tau_2)}{\hbar(\tau_1)\Gamma(\tau_1 + \tau_2)} \right) \|u - u_1\|, \\ |v - v_1| &\leq v_5 \omega_5, \text{ with } v_5 = \left(\frac{\tau_2(1-\tau_1)}{\hbar(\tau_1)} + \frac{\tau_1\tau_2\Gamma(\tau_2)}{\hbar(\tau_1)\Gamma(\tau_1 + \tau_2)} \right) \|v - v_1\|. \end{aligned}$$

Hence, the results follows. \square

3.4. Sensitivity analysis

According to the parameters of our model, the following equation yields the sensitivity index of \mathcal{R}_0 :

$$\Gamma_{\omega}^{\mathcal{R}_0} = \frac{\partial \mathcal{R}_0}{\partial \omega} \times \frac{\omega}{\mathcal{R}_0}, \quad (3.5)$$

where ω is a value from Table 1. Table 1 lists the sensitivity indices of \mathcal{R}_0 . It is easy to verify that

$$\frac{\partial \mathcal{R}_0}{\partial \varrho} = \frac{[\mathbf{b}\chi + \mathbf{a}(\alpha + \eta + \mu) - (\mathbf{a}\eta(1 - \mathbf{q}) + \mathbf{b}(\beta + \chi + \mu))]}{(\beta + \chi + \mu)(\alpha + \eta + \mu) - \eta(1 - \mathbf{q})\chi} (x_0 + \varepsilon y_0) = -0.0025 < 0,$$

$$\begin{aligned} \frac{\partial \mathcal{R}_0}{\partial \mu} &= \frac{(\mathbf{a}\varrho + \mathbf{b}(1 - \varrho))((\beta + \chi + \mu)(\alpha + \eta + \mu) - \eta(1 - \mathbf{q})\chi)}{((\beta + \chi + \mu)(\alpha + \eta + \mu) - \eta(1 - \mathbf{q})\chi)^2} (x_0 + \varepsilon y_0) \\ &\quad - \frac{[\varrho(\mathbf{b}\chi + \mathbf{a}(\alpha + \eta + \mu)) + (1 - \varrho)(\mathbf{a}\eta(1 - \mathbf{q}) + \mathbf{b}(\beta + \chi + \mu))](2\alpha + \eta + \mu + \beta + \chi)}{((\beta + \chi + \mu)(\alpha + \eta + \mu) - \eta(1 - \mathbf{q})\chi)^2} (x_0 + \varepsilon y_0) \\ &= 1.1058 > 0, \end{aligned}$$

$$\begin{aligned} \frac{\partial \mathcal{R}_0}{\partial \alpha} &= \frac{(\mathbf{a}\varrho(\beta + \chi + \mu)(\alpha + \eta + \mu) - \mathbf{a}\varrho\eta(1 - \mathbf{q})\chi)}{((\beta + \chi + \mu)(\alpha + \eta + \mu) - \eta(1 - \mathbf{q})\chi)^2} (x_0 + \varepsilon y_0) \\ &\quad - \frac{[\varrho(\mathbf{b}\chi + \mathbf{a}(\alpha + \eta + \mu)) + (1 - \varrho)(\mathbf{a}\eta(1 - \mathbf{q}) + \mathbf{b}(\beta + \chi + \mu))](\beta + \chi + \mu)}{((\beta + \chi + \mu)(\alpha + \eta + \mu) - \eta(1 - \mathbf{q})\chi)^2} (x_0 + \varepsilon y_0) \\ &= -0.1418 < 0, \end{aligned}$$

$$\begin{aligned} \frac{\partial \mathcal{R}_0}{\partial \eta} &= \frac{\mathbf{a}(\varrho + (1 - \varrho)(1 - \mathbf{q}))((\beta + \chi + \mu)(\alpha + \eta + \mu) - \eta(1 - \mathbf{q})\chi)}{((\beta + \chi + \mu)(\alpha + \eta + \mu) - \eta(1 - \mathbf{q})\chi)^2} (x_0 + \varepsilon y_0) \\ &\quad - \frac{[\varrho(\mathbf{b}\chi + \mathbf{a}(\alpha + \eta + \mu)) + (1 - \varrho)(\mathbf{a}\eta(1 - \mathbf{q}) + \mathbf{b}(\beta + \chi + \mu))](\beta + \chi + \mu - (1 - \mathbf{q})\chi)}{((\beta + \chi + \mu)(\alpha + \eta + \mu) - \eta(1 - \mathbf{q})\chi)^2} (x_0 + \varepsilon y_0) \\ &= -0.0662 < 0, \end{aligned}$$

$$\begin{aligned} \frac{\partial \mathcal{R}_0}{\partial \beta} &= \frac{\mathbf{b}(1 - \varrho)((\beta + \chi + \mu)(\alpha + \eta + \mu) - \eta(1 - \mathbf{q})\chi)}{((\beta + \chi + \mu)(\alpha + \eta + \mu) - \eta(1 - \mathbf{q})\chi)^2} (x_0 + \varepsilon y_0) \\ &\quad - \frac{[\varrho(\mathbf{b}\chi + \mathbf{a}(\alpha + \eta + \mu)) + (1 - \varrho)(\mathbf{a}\eta(1 - \mathbf{q}) + \mathbf{b}(\beta + \chi + \mu))](\alpha + \eta + \mu)}{((\beta + \chi + \mu)(\alpha + \eta + \mu) - \eta(1 - \mathbf{q})\chi)^2} (x_0 + \varepsilon y_0) \\ &= -0.1938 < 0, \end{aligned}$$

$$\begin{aligned} \frac{\partial \mathcal{R}_0}{\partial \chi} &= \frac{b((\beta + \chi + \mu)(\alpha + \eta + \mu) - \eta(1 - q)\chi)}{((\beta + \chi + \mu)(\alpha + \eta + \mu) - \eta(1 - q)\chi)^2} (x_0 + \varepsilon y_0) \\ &\quad - \frac{[\varrho(b\chi + a(\alpha + \eta + \mu)) + (1 - \varrho)(a\eta(1 - q) + b(\beta + \chi + \mu))](\alpha + \eta + \mu - \eta(1 - q))}{((\beta + \chi + \mu)(\alpha + \eta + \mu) - \eta(1 - q)\chi)^2} (x_0 + \varepsilon y_0) \\ &= 0.0835 > 0, \end{aligned}$$

$$\begin{aligned} \frac{\partial \mathcal{R}_0}{\partial q} &= \frac{-(a(1 - \varrho)\eta)((\beta + \chi + \mu)(\alpha + \eta + \mu) - \eta(1 - q)\chi)}{((\beta + \chi + \mu)(\alpha + \eta + \mu) - \eta(1 - q)\chi)^2} (x_0 + \varepsilon y_0) \\ &\quad - \frac{[\varrho(b\chi + a(\alpha + \eta + \mu)) + (1 - \varrho)(a\eta(1 - q) + b(\beta + \chi + \mu))](\eta\chi)}{((\beta + \chi + \mu)(\alpha + \eta + \mu) - \eta(1 - q)\chi)^2} (x_0 + \varepsilon y_0) \\ &= -0.0052 < 0, \end{aligned}$$

$$\frac{\partial \mathcal{R}_0}{\partial a} = \frac{(\varrho(\alpha + \eta + \mu) + (1 - \varrho)\eta(1 - q))}{((\beta + \chi + \mu)(\alpha + \eta + \mu) - \eta(1 - q)\chi)} (x_0 + \varepsilon y_0) = 2.2216 > 0,$$

$$\frac{\partial \mathcal{R}_0}{\partial b} = \frac{(\varrho\chi + (1 - \varrho)(\beta + \chi + \mu))}{((\beta + \chi + \mu)(\alpha + \eta + \mu) - \eta(1 - q)\chi)} (x_0 + \varepsilon y_0) = 3.9229 > 0,$$

$$\frac{\partial \mathcal{R}_0}{\partial \varepsilon} = \frac{y_0[\varrho(b\chi + a(\alpha + \eta + \mu)) + (1 - \varrho)(a\eta(1 - q) + b(\beta + \chi + \mu))]}{(\beta + \chi + \mu)(\alpha + \eta + \mu) - \eta(1 - q)\chi} = 0.0025 > 0.$$

The sensitivity index of each parameter in the model obtained as in Table 1 by applying (3.5). The sensitivity indexes of Table 1 indicate that \mathcal{R}_0 increases as the parameters χ , μ , a , b and ε are increased. In contrast, the values of other parameters are fixed. Based on these indices, it appears that disease endemicity has increased. In contrast, when the parameters β , η , q , α and ϱ are decreased while the rest of the parameters are maintained, \mathcal{R}_0 decreases.

4. Numerical procedures

Atangana-Baleanu fractal-fractional operators are implemented via Lagrangian piecewise interpolation for the proposed model.

4.1. Adams-Bashforth-Moulton method application

As in [82, 83], consider system (2.2) in the following case:

$${}^z \mathcal{D}_{0,t}^{\tau_1} \Psi(\mathbf{t}) = \Lambda(\mathbf{t}, \Psi(\mathbf{t})),$$

subject to ceil function $n = [\tau_1]$ and for $t \in [0, T]$, $0 < \tau_1 \leq 1$ with ${}^Z \mathcal{D}_{0,t}^{\tau_1} \Psi(0) = \Psi_0^{(\kappa)}$, $\kappa = 0, 1, 2, \dots, n-1$. Volterra's integral equation of system (2.3) is given by

$$\Psi = \sum_{\kappa=0}^{n-1} \frac{t^\kappa}{\kappa!} \Psi_0^{(\kappa)} + \frac{1}{\Gamma(\tau_1)} \int_0^t (t-\xi)^{\tau_1-1} \Lambda(\xi, \Psi(\xi)) d\xi. \quad (4.1)$$

It is easy to reconstruct Eq (4.1) by using the product rule for rectangles,

$$\int_0^{t_{n+1}} (t_{n+1} - \xi)^{\tau_1-1} \Lambda(\xi, \Psi(\xi)) d\xi \simeq \sum_{\kappa=0}^n \Psi_{\kappa,n+1} \Lambda(t_\kappa, g_h(t_\kappa)),$$

where $\mathbb{A}_{\kappa,n+1}$ is given by

$$\mathbb{A}_{\kappa,n+1} = \begin{cases} n^{\tau_1+1} - (n - \tau_1)(n + 1)^{\tau_1} & \text{if } \kappa = 0, \\ (n - \kappa + 2)^{\tau_1+1} + (n - \kappa)^{\tau_1+1} - 2(n - \kappa + 1)^{\tau_1+1} & \text{if } 1 \leq \kappa \leq n, \\ 1 & \text{if } \kappa = n + 1. \end{cases}$$

Let $\{t_n = nh : n = -k, -k + 1, \dots, -1, 0, 1, \dots, N\}$, with $h = T/N$. Then, (4.1) can be discretized as follows:

$$\Psi_h(t_{n+1}) = \sum_{\kappa=0}^{n-1} \frac{t_{n+1}^\kappa}{\kappa!} \Psi_0^{(\kappa)} + \frac{h^{\tau_1}}{\Gamma(\tau_1 + 2)} \Lambda(t_{n+1}, \Psi(t_{n+1})) + \frac{h^{\tau_1}}{\Gamma(\tau_1 + 2)} \sum_{\kappa=0}^n \mathbb{A}_{\kappa,n+1} \Lambda(t_\kappa, \Psi(t_\kappa)). \quad (4.2)$$

The predicted value $\Psi_h^p(t_{n+1})$ is determined as follows:

$$\Psi_h^p(t_{n+1}) = \sum_{\kappa=0}^{\ell-1} \frac{t_{n+1}^\kappa}{\kappa!} \Psi_0^{(\kappa)} + \frac{1}{\Gamma(\tau_1)} \sum_{\kappa=0}^n \mathbb{B}_{\kappa,n+1} \Lambda(t_\kappa, \Psi(t_\kappa)),$$

where

$$\mathbb{B}_{\kappa,n+1} = \frac{h^{\tau_1}}{\tau_1} ((n - \kappa + 1)^{\tau_1} - (n - \kappa)^{\tau_1}), \quad \text{if } 1 \leq \kappa \leq n.$$

According to (4.2), (2.1) is as follows:

$$\begin{aligned}
 x_{n+1} &= x_0 + \frac{h^{\tau_1}}{\Gamma(\tau_1 + 2)} \left[(1 - p)\pi + \phi y_{n+1}^p + \delta v_{n+1}^p - (\vartheta + \mu + \lambda) x_{n+1}^p \right] \\
 &\quad + \frac{h^{\tau_1}}{\Gamma(\tau_1 + 2)} \sum_{\kappa=0}^n \mathbb{A}_{\kappa, n+1} [(1 - p)\pi + \phi y_{\kappa} + \delta w_{\kappa} - (\vartheta + \mu + \lambda) x_{\kappa}], \\
 y_{n+1} &= y_0 + \frac{h^{\tau_1}}{\Gamma(\tau_1 + 2)} \left[p\pi + \vartheta x_{n+1}^p - (\phi + \mu + \varepsilon\lambda) y_{n+1}^p \right] \\
 &\quad + \frac{h^{\tau_1}}{\Gamma(\tau_1 + 2)} \sum_{\kappa=0}^n \mathbb{A}_{\kappa, n+1} [p\pi + \vartheta x_{\kappa} - (\phi + \mu + \varepsilon\lambda) y_{\kappa}], \\
 z_{n+1} &= z_0 + \frac{h^{\tau_1}}{\Gamma(\tau_1 + 2)} \left[\varrho\lambda x_{n+1}^p + \varrho\varepsilon\lambda y_{n+1}^p + \eta(1 - q)u_{n+1}^p - (\beta + \chi + \mu) z_{n+1}^p \right] \\
 &\quad + \frac{h^{\tau_1}}{\Gamma(\tau_1 + 2)} \sum_{\kappa=0}^n \mathbb{A}_{\kappa, n+1} [\varrho\lambda x_{\kappa} + \varrho\varepsilon\lambda y_{\kappa} + \eta(1 - q)u_{\kappa} - (\beta + \chi + \mu) z_{\kappa}], \\
 u_{n+1} &= u_0 + \frac{h^{\tau_1}}{\Gamma(\tau_1 + 2)} \left[\lambda(1 - \varrho) x_{n+1}^p + \varepsilon\lambda(1 - \varrho) y_{n+1}^p + \chi z_{n+1}^p - (\alpha + \eta + \mu) u_{n+1}^p \right] \\
 &\quad + \frac{h^{\tau_1}}{\Gamma(\tau_1 + 2)} \sum_{\kappa=0}^n \mathbb{A}_{\kappa, n+1} [\lambda(1 - \varrho) x_{\kappa} + \varepsilon\lambda(1 - \varrho) y_{\kappa} + \chi z_{\kappa} - (\alpha + \eta + \mu) u_{\kappa}], \\
 v_{n+1} &= v_0 + \frac{h^{\tau_1}}{\Gamma(\tau_1 + 2)} \left[\beta z_{n+1}^p + q\eta u_{n+1}^p - (\delta + \mu) v_{n+1}^p \right] \\
 &\quad + \frac{h^{\tau_1}}{\Gamma(\tau_1 + 2)} \sum_{\kappa=0}^n \mathbb{A}_{\kappa, n+1} [\beta z_{\kappa} + q\eta u_{\kappa} - (\delta + \mu) v_{\kappa}],
 \end{aligned}$$

where

$$\begin{aligned}
 x_{n+1}^p &= x_0 + \frac{h^{\tau_1}}{\Gamma(\tau_1 + 2)} \sum_{\kappa=0}^n \mathbb{B}_{\kappa, n+1} [(1 - p)\pi + \phi y_{\kappa} + \delta w_{\kappa} - (\vartheta + \mu + \lambda) x_{\kappa}], \\
 y_{n+1}^p &= y_0 + \frac{h^{\tau_1}}{\Gamma(\tau_1 + 2)} \sum_{\kappa=0}^n \mathbb{B}_{\kappa, n+1} [p\pi + \vartheta x_{\kappa} - (\phi + \mu + \varepsilon\lambda) y_{\kappa}], \\
 z_{n+1}^p &= z_0 + \frac{h^{\tau_1}}{\Gamma(\tau_1 + 2)} \sum_{\kappa=0}^n \mathbb{B}_{\kappa, n+1} [\varrho\lambda x_{\kappa} + \varrho\varepsilon\lambda y_{\kappa} + \eta(1 - q)u_{\kappa} - (\beta + \chi + \mu) z_{\kappa}], \\
 u_{n+1}^p &= u_0 + \frac{h^{\tau_1}}{\Gamma(\tau_1 + 2)} \sum_{\kappa=0}^n \mathbb{B}_{\kappa, n+1} [\lambda(1 - \varrho) x_{\kappa} + \varepsilon\lambda(1 - \varrho) y_{\kappa} + \chi z_{\kappa} - (\alpha + \eta + \mu) u_{\kappa}], \\
 v_{n+1}^p &= v_0 + \frac{h^{\tau_1}}{\Gamma(\tau_1 + 2)} \sum_{\kappa=0}^n \mathbb{B}_{\kappa, n+1} [\beta z_{\kappa} + q\eta u_{\kappa} - (\delta + \mu) v_{\kappa}].
 \end{aligned}$$

4.2. Application of the fractal-fractional Atangana-Baleanu scheme

$${}^{\text{FF-AB}}\mathcal{D}_{0,t}^{\tau_1, \tau_2} \Psi(t) = \Lambda(t, \Psi(t)).$$

The Antangana-Baleanu integral gives us

$$\vartheta(t) = \Psi(0) + \frac{1 - \tau_1}{\hbar(\tau_1)} \Lambda(t, \Psi(t)) + \frac{\tau_1}{\hbar(\tau_1)\Gamma(\tau_1)} \int_0^t (t - \xi)^{\tau_1 - 1} \xi^{\tau_2 - 1} \Lambda(\xi, \Psi(\xi)) d\xi.$$

Replacing t with t_{n+1} we have

$$\Psi^{n+1} = \Psi(0) + \frac{1 - \tau_1}{\hbar(\tau_1)} \Lambda(t_{n+1}, \Psi(t)) + \frac{\tau_1}{\hbar(\tau_1)\Gamma(\tau_1)} \int_0^{t_{n+1}} (t_{n+1} - \xi)^{\tau_1 - 1} \xi^{\tau_2 - 1} \Lambda(\xi, \Psi(\xi)) d\xi.$$

Application of the two-step Lagrange polynomial yields

$$\begin{aligned} \Lambda(t, (y, \Psi(t))) &= \frac{(y - t_{\xi-1}) \Lambda(t, (t_\xi, \Psi(t_\xi))) - (y - t_\xi) \Lambda(t_{\xi-1}, \Psi(t_{\xi-1}))}{t_\xi - t_{\xi-1}} \\ &= \frac{\Lambda(t, (t_\xi, \Psi(t_\xi))) (x - t_{\xi-1}) - \Lambda(t_{\xi-1}, \Psi(t_{\xi-1})) (y - t_\xi)}{t_\xi - t_{\xi-1}} \\ &= \frac{\Lambda(t, (t_\xi, \Psi(t_\xi))) (y - t_{\xi-1}) - \Lambda(t_{\xi-1}, \Psi(t_{\xi-1})) (y - t_\xi)}{h}. \end{aligned}$$

By using the Lagrange polynomial to solve the given problem, we obtain

$$\begin{aligned} \Psi^{n+1} &= \Psi(0) + \frac{1 - \tau_1}{\hbar(\tau_1)} \Lambda(t, (t_n, \Psi(t_n))) \\ &+ \frac{\tau_1}{\hbar(\tau_1)\Gamma(\tau_1)} \sum_{\xi=1}^n \left(\frac{\Lambda(t, (t_\xi, \Psi(t_\xi)))}{h} \int_{t_\xi}^{t_{\xi+1}} (\xi - t_\xi - 1) (t_{n+1} - \xi)^{\tau_1 - 1} d\xi \right. \\ &\left. - \frac{\Lambda(t, (t_{\xi-1}, \Psi(t_{\xi-1})))}{h} \int_{t_\xi}^{t_{n+1}} (\xi - t_\xi) (t_{n+1} - \xi)^{\tau_1 - 1} d\xi \right). \end{aligned}$$

Now, solving the integral we get

$$\begin{aligned} \Psi^{n+1} &= \Psi(0) + \frac{1 - \tau_1}{\hbar(\tau_1)} \Lambda(t, (t_n, \Psi(t_n))) + \frac{\tau_1 h^{\tau_1}}{\Gamma(\tau_1 + 2)} \\ &\times \sum_{\xi=1}^n \left[\Lambda(t, (t_\xi, \Psi(t_\xi))) ((n - \xi + 1)^{\tau_1} (n - \xi + 2 + \tau_1) - (n - \xi)^{\tau_1} (n - \xi + 2 + 2\tau_1)) \right. \\ &\left. - \Lambda(t, (t_{\xi-1}, \Psi_{\xi-1})) ((n - \xi + 1)^{\tau_1 + 1} - (n - \xi + 1 + \tau_1) (n - \xi)^{\tau_1}) \right]. \end{aligned}$$

Now, replacing the value of $\Lambda(y, \Psi(t))$, we get

$$\begin{aligned} \Psi^{n+1} &= \Psi(0) + \tau_2 t^{\tau_2 - 1} \frac{1 - \tau_1}{\hbar(\tau_1)} \Lambda(t_\xi, \Psi(t_\xi)) + \tau_2 t^{\tau_2 - 1} \frac{\tau_1 h^{\tau_1}}{\Gamma(\tau_1 + 2)} \\ &\times \sum_{\xi=1}^n \left[\Lambda(t_\xi, \Psi(t_\xi)) ((n + 1 - \xi)^{\tau_1} (n - \xi + 2 + \tau_1) - (n - \xi)^{\tau_1} (n - \xi + 2 + 2\tau_1)) \right. \\ &\left. - \Lambda(t_{\xi-1}, \Psi_{\xi-1}) ((n - \xi + 1)^{\tau_1 + 1} - (n - \xi + 1 + \tau_1) (n - \xi)^{\tau_1}) \right]. \end{aligned}$$

As a result, the numerical scheme above rewritten as follows:

$$\begin{aligned} x^{n+1} &= x(0) + \tau_2 t^{\tau_2-1} \frac{1-\tau_1}{\hbar(\tau_1)} \Upsilon_1(t_\xi, x(t_\xi)) + \tau_2 t^{\tau_2-1} \frac{\tau_1 h^{\tau_1}}{\Gamma(\tau_1+2)} \\ &\times \sum_{\xi=1}^n \left[\Upsilon_1(t_\xi, x(t_\xi)) ((n-\xi+1)^{\tau_1} (n-\xi+2+\tau_1) - (n-\xi)^{\tau_1} (n-\xi+2+2\tau_1)) \right. \\ &\left. - \Upsilon_1(t_{\xi-1}, x_{\xi-1}) ((n-\xi+1)^{\tau_1+1} - (n-\xi+1+\tau_1)(n-\xi)^{\tau_1}) \right], \end{aligned}$$

$$\begin{aligned} y^{n+1} &= y(0) + \tau_2 t^{\tau_2-1} \frac{1-\tau_1}{\hbar(\tau_1)} \Upsilon_2(t_\xi, y(t_\xi)) + \tau_2 t^{\tau_2-1} \frac{\tau_1 h^{\tau_1}}{\Gamma(\tau_1+2)} \\ &\times \sum_{\xi=1}^n \left[\Upsilon_2(t_\xi, y(t_\xi)) ((n-\xi+1)^{\tau_1} (n-\xi+2+\tau_1) - (n-\xi)^{\tau_1} (n-\xi+2+2\tau_1)) \right. \\ &\left. - \Upsilon_2(t_{\xi-1}, y_{\xi-1}) ((n-\xi+1)^{\tau_1+1} - (n-\xi+1+\tau_1)(n-\xi)^{\tau_1}) \right], \end{aligned}$$

$$\begin{aligned} z^{n+1} &= z(0) + \tau_2 t^{\tau_2-1} \frac{1-\tau_1}{\hbar(\tau_1)} \Upsilon_3(t_\xi, z(t_\xi)) + \tau_2 t^{\tau_2-1} \frac{\tau_1 h^{\tau_1}}{\Gamma(\tau_1+2)} \\ &\times \sum_{\xi=1}^n \left[\Upsilon_3(t_\xi, z(t_\xi)) ((n-\xi+1)^{\tau_1} (n-\xi+2+\tau_1) - (n-\xi)^{\tau_1} (n-\xi+2+2\tau_1)) \right. \\ &\left. - \Upsilon_3(t_{\xi-1}, z_{\xi-1}) ((n-\xi+1)^{\tau_1+1} - (n-\xi+1+\tau_1)(n-\xi)^{\tau_1}) \right], \end{aligned}$$

$$\begin{aligned} u^{n+1} &= u(0) + \tau_2 t^{\tau_2-1} \frac{1-\tau_1}{\hbar(\tau_1)} \Upsilon_4(t_\xi, u(t_\xi)) + \tau_2 t^{\tau_2-1} \frac{\tau_1 h^{\tau_1}}{\Gamma(\tau_1+2)} \\ &\times \sum_{\xi=1}^n \left[\Upsilon_4(t_\xi, u(t_\xi)) ((n-\xi+1)^{\tau_1} (n-\xi+2+\tau_1) - (n-\xi)^{\tau_1} (n-\xi+2+2\tau_1)) \right. \\ &\left. - \Upsilon_4(t_{\xi-1}, u_{\xi-1}) ((n-\xi+1)^{\tau_1+1} - (n-\xi+1+\tau_1)(n-\xi)^{\tau_1}) \right], \end{aligned}$$

$$\begin{aligned} v^{n+1} &= v(0) + \tau_2 t^{\tau_2-1} \frac{1-\tau_1}{\hbar(\tau_1)} \Upsilon_5(t_\xi, v(t_\xi)) + \tau_2 t^{\tau_2-1} \frac{\tau_1 h^{\tau_1}}{\Gamma(\tau_1+2)} \\ &\times \sum_{\xi=1}^n \left[\Upsilon_5(t_\xi, v(t_\xi)) ((n-\xi+1)^{\tau_1} (n-\xi+2+\tau_1) - (n-\xi)^{\tau_1} (n-\xi+2+2\tau_1)) \right. \\ &\left. - \Upsilon_5(t_{\xi-1}, v_{\xi-1}) ((n-\xi+1)^{\tau_1+1} - (n-\xi+1+\tau_1)(n-\xi)^{\tau_1}) \right]. \end{aligned}$$

Table 2. Sensitivity index of the applied parameters.

Parameters	Sensitivity index
β	-0.4669
η	-0.3987
q	-0.1264
α	-0.0973
ϱ	-0.0035
χ	0.0101
μ	0.1332
a	0.2676
b	0.9450
ϵ	$5.9220 \times e^{-04}$

4.3. Numerical simulations and discussion

The above analyses are displayed in Figures 2–16, which display the time series of the model (2.1) under the following initial conditions: $x(0) = 8200, y(0) = 2800, z(0) = 200, u(0) = 210, v(0) = 200$. Figures 2–6 show that the time series of the model (2.1) with different trajectories of infected states tends to zero whenever $R_0 = 0.0083 < 1$. The proposed model was simulated for approximately 100 days for different fractal fractional-order values τ_1 and τ_2 . According to these parameters, $E_0 = (0.1192, 0.2961, 0, 0, 0)$ is asymptotically stable. As predicted, the solutions of (2.1) converge to the unique disease-free equilibrium E_0 . The biological implication is that we need to bring R_0 to below 1 to ensure a reduction of the disease in the country.

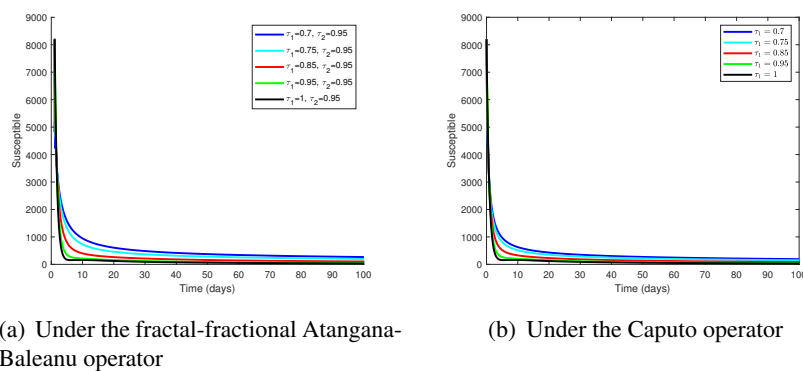
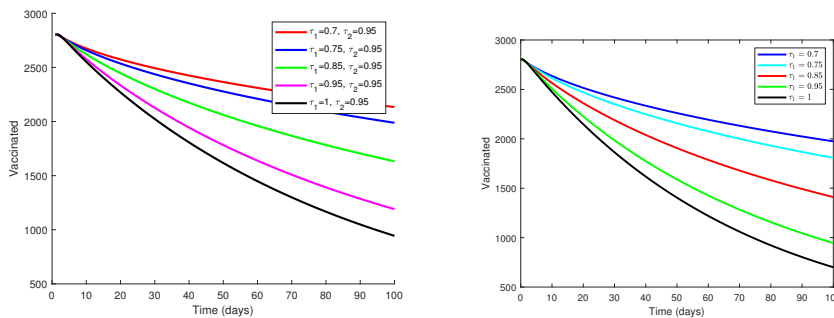
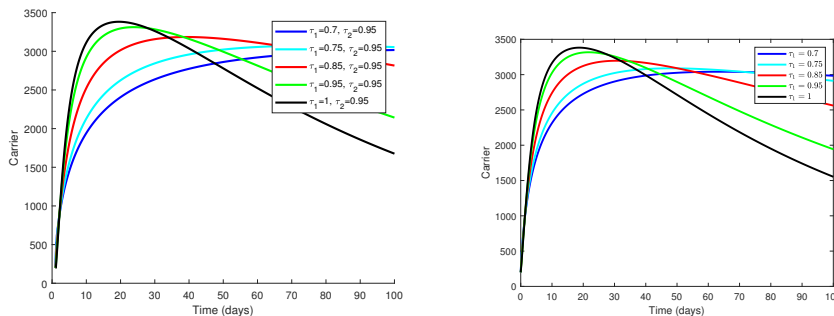


Figure 2. For $R_0 = 0.0083 < 1$ with different fractional-order τ_1 values with a fixed $\tau_2 = 0.95$, a time series plot of the susceptible (x) is shown.



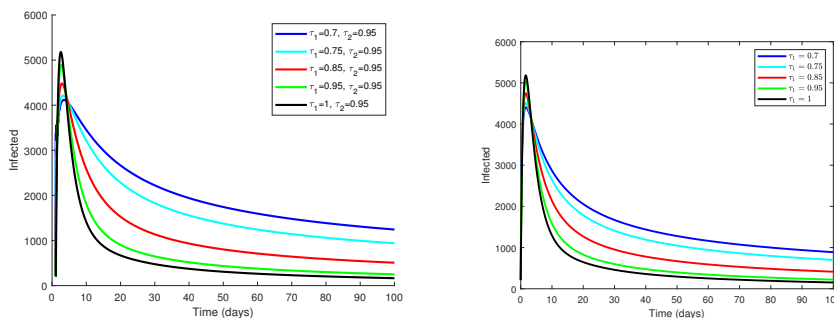
(a) Under the fractal-fractional Atangana-Baleanu operator (b) Under the Caputo operator

Figure 3. For $\mathcal{R}_0 = 0.0083 < 1$ with different fractional-order τ_1 values with a fixed $\tau_2 = 0.95$, a time series plot of the vaccinated (y) is shown.



(a) Under the fractal-fractional Atangana-Baleanu operator (b) Under the Caputo operator

Figure 4. For $\mathcal{R}_0 = 0.0083 < 1$ with different fractional-order τ_1 values with a fixed $\tau_2 = 0.95$, a time series plot of the carrier (z) is shown.



(a) Under the fractal-fractional Atangana-Baleanu operator (b) Under the Caputo operator

Figure 5. For $\mathcal{R}_0 = 0.0083 < 1$ with different fractional-order τ_1 values with a fixed $\tau_2 = 0.95$, a time series plot of the infected (u) is shown.

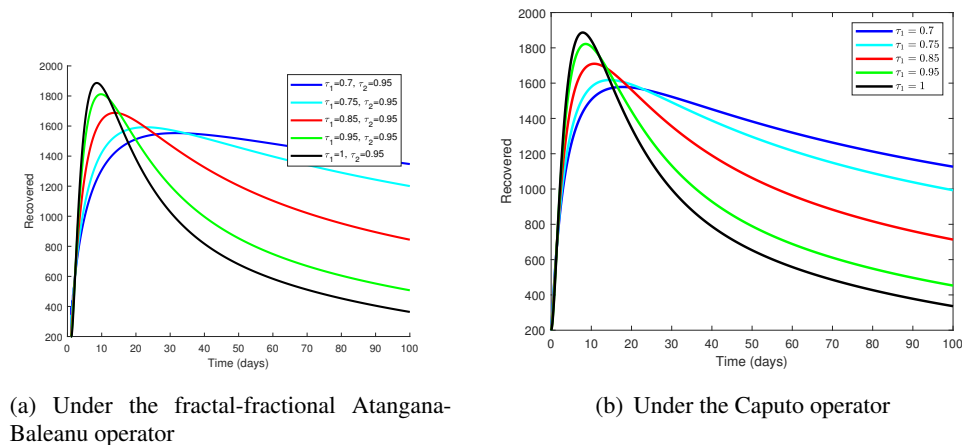


Figure 6. For $\mathcal{R}_0 = 0.0083 < 1$ with different fractional-order τ_1 values with a fixed $\tau_2 = 0.95$, a time series plot of the recovered (v) is shown.

Figures 2–6 show the results of the fractal-fractional Atangana-Baleanu and the Adams-Bashforth-Moulton methods for pneumonia transmission, with (a) $\tau_1 = 0.7, \tau_2 = 0.95$, (b) $\tau_1 = 0.75, \tau_2 = 0.95$, (c) $\tau_1 = 0.85, \tau_2 = 0.95$ (d) $\tau_1 = 0.95, \tau_2 = 0.95$ and (e) $\tau_1 = 1, \tau_2 = 0.95$. Comparisons between the ordinary differential system, ABC fractal, and fractional derivative, can also be seen in Figures 2–6.

Figures 2–6 show the influence of varying τ_1 between 0.7 and 1 with a fixed $\tau_2 = 0.95$ on model dynamics. The black curve in each of these figures represents the numerical results of model (2.1) when the fractional order is equal to 1. From the results of Figures 2–6, it follows that the variation of the fractional parameter has a great impact on the quantitative dynamics of the model. Indeed, in Figure 5, the classes of infected humans peak after 10 years and decrease according to the decrease of the fractional parameter τ_1 .

Lemmas 2 and 3 are validated numerically in Figures 2–6. It is clear that varying the fractional order parameter τ_1 does not influence the model dynamics whenever $\mathcal{R}_0 = 0.0083 < 1$. Indeed, whatever the value of τ_1 , the infected compartments tend to zero asymptotically whenever $\mathcal{R}_0 = 0.0083 < 1$. This validates the fact that the pneumonia-free equilibrium of the fractional model is globally asymptotically stable whenever $\mathcal{R}_0 = 0.0083 < 1$.

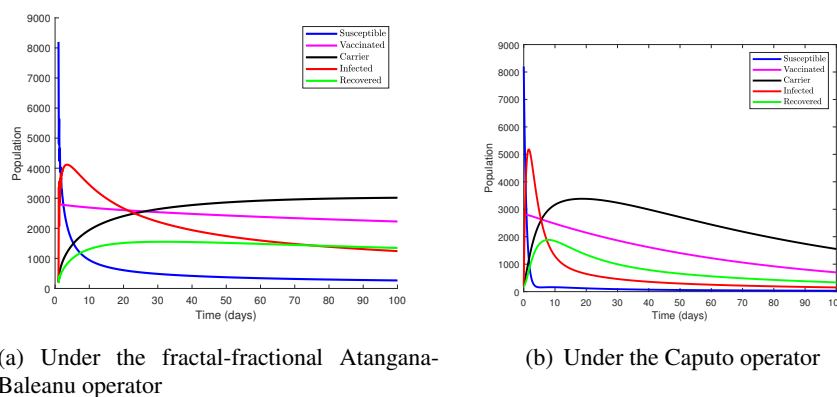
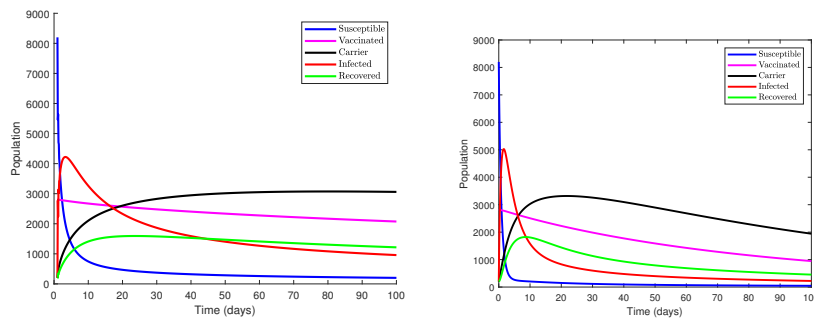


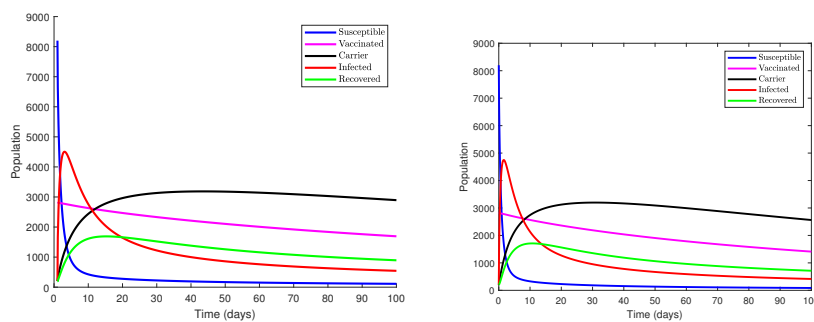
Figure 7. Dynamics of system (2.1) for (a) $\tau_1 = 0.7, \tau_2 = 0.95$, (b) $\tau_1 = 0.7$.



(a) Under the fractal-fractional Atangana-Baleanu operator

(b) Under the Caputo operator

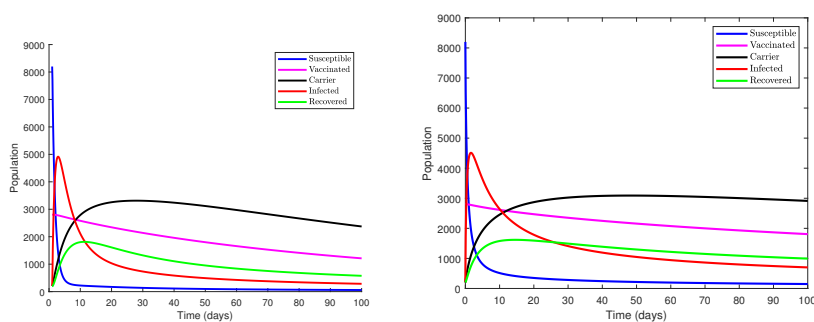
Figure 8. Dynamics of system (2.1) for (a) $\tau_1 = 0.75, \tau_2 = 0.95$, (b) $\tau_1 = 0.75$.



(a) Under the fractal-fractional Atangana-Baleanu operator

(b) Under the Caputo operator

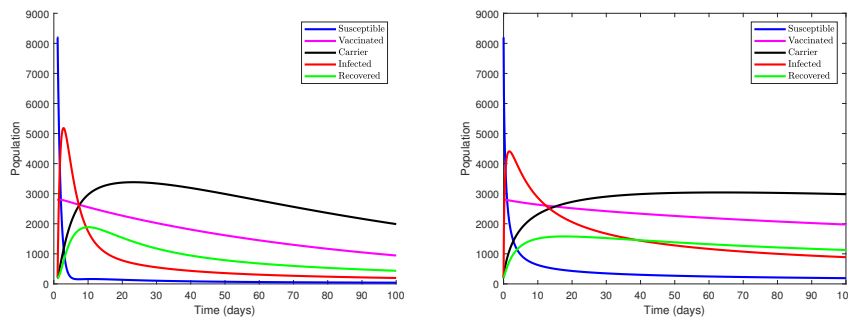
Figure 9. Dynamics of system (2.1) for (a) $\tau_1 = 0.85, \tau_2 = 0.95$, (b) $\tau_1 = 0.85$.



(a) Under the fractal-fractional Atangana-Baleanu operator

(b) Under the Caputo operator

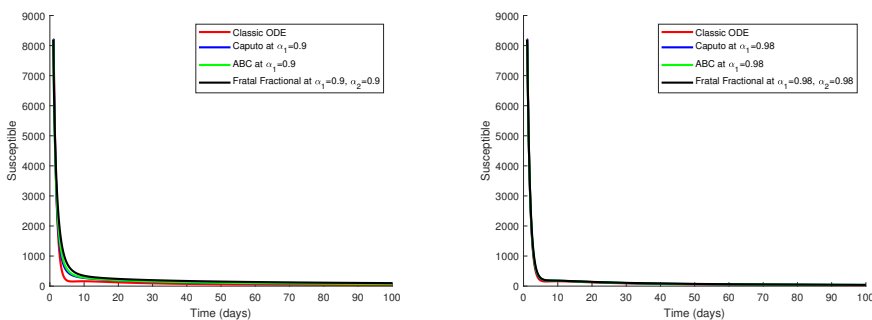
Figure 10. Dynamics of system (2.1) for (a) $\tau_1 = 0.95, \tau_2 = 0.95$, (b) $\tau_1 = 0.95$.



(a) Under the fractal-fractional Atangana-Baleanu operator (b) Under the Caputo operator

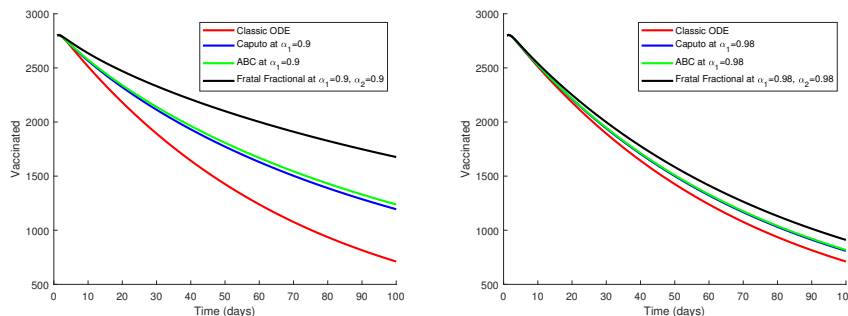
Figure 11. Dynamics of all five compartments for (a) $\tau_1 = 1, \tau_2 = 0.95$, (b) $\tau_1 = 1$.

Figures 7–11 show the phase plots $(x - y - z - u - v)$ for different values, i.e., (a) $\tau_1 = 0.7, \tau_2 = 0.95$, (b) $\tau_1 = 0.75, \tau_2 = 0.95$, (c) $\tau_1 = 0.85, \tau_2 = 0.95$ (d) $\tau_1 = 0.95, \tau_2 = 0.95$ and (e) $\tau_1 = 1, \tau_2 = 0.95$.



(a) (b)

Figure 12. Comparison between the three numerical schemes: ODE, Caputo and fractal-fractional in two cases (a) and (b).



(a) (b)

Figure 13. Comparison between the three numerical schemes: ODE, Caputo and fractal-fractional in two cases (a) and (b).

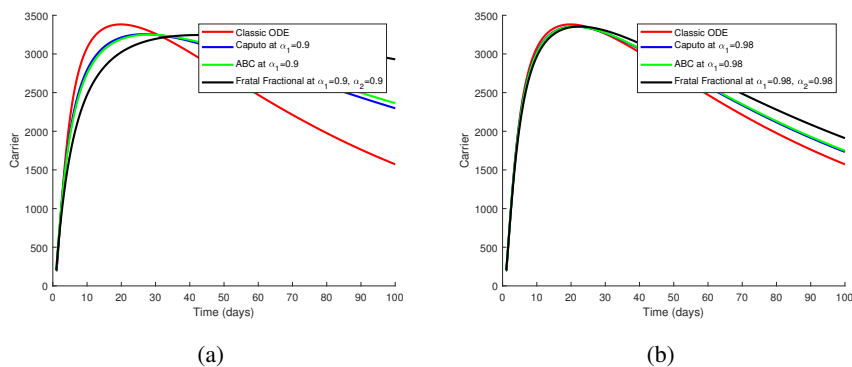


Figure 14. Comparison between the three numerical schemes: ODE, Caputo and fractal-fractional in two cases (a) and (b).

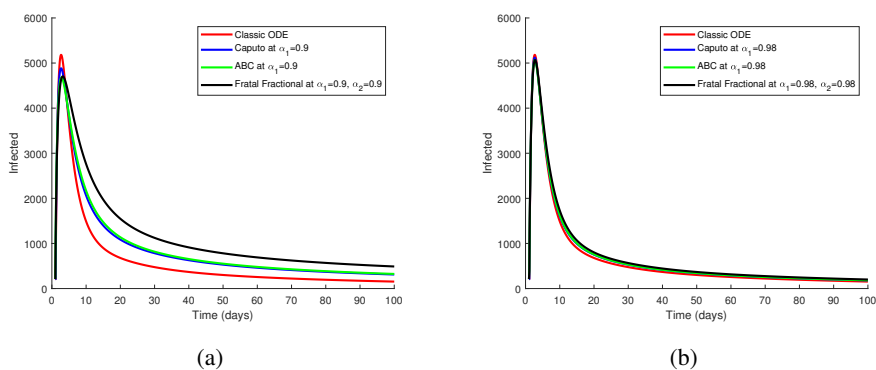


Figure 15. Comparison between the three numerical schemes: ODE, Caputo and fractal-fractional in two cases (a) and (b).

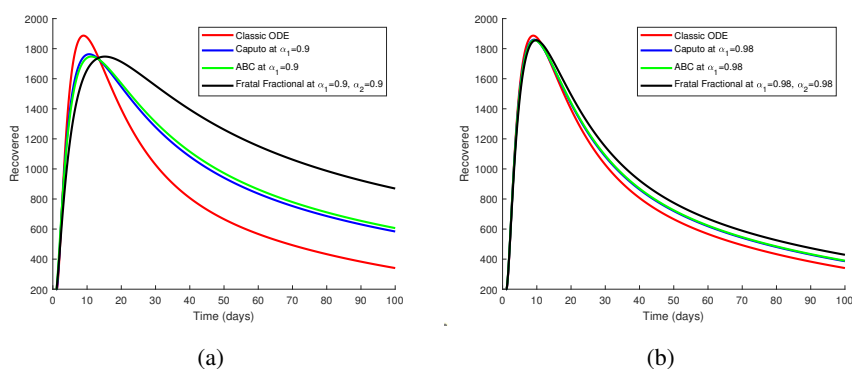


Figure 16. Comparison between the three numerical schemes: ODE, Caputo and fractal-fractional in two cases (a) and (b).

Comparison between ordinary differential system, ABC, ABC fractal fractional derivative schemes can be seen in Figures 12–16.

5. Conclusions

A fractal fractional-order mathematical model based on the Atangana-Baleanu operator was constructed to describe pneumonia transmission in a population. The Caputo operator was used to analyze the dynamics of the virus, and a fractal fractional derivative was used to maximize the number of recovered populations. For models of infectious diseases, the vaccination rate coefficient is considered as a control to reduce the disease burden. It is important to prove the existence of optimal control, characterize the optimal control, prove the uniqueness of optimal control and compute the optimal control numerically. The model was subjected to dynamic analysis, and the results show that the rate at which susceptible individuals contract an infectious disease is the most significant parameter. In this simulation, the value of $\mathcal{R}_0 = 0.0083 < 1$, which is smaller than 1. As you can see, disease spread is controlled, and the number of infected people is reduced to zero. We also see that each function tends to its equilibrium point, and that the equilibrium point becomes stable as the system approaches its equilibrium point. We also note that the total number of susceptible humans decreases rapidly according to the increase of the fractional parameter (Figure 2).

Use of AI tools declaration

The authors declare they have not used Artificial Intelligence (AI) tools in the creation of this article.

Acknowledgments

The authors gratefully acknowledge Qassim University, represented by the Deanship of Scientific Research, for the financial support for this research under grant number (37622-BSRC-FFT-2023) during the academic year 1445 AH/2023 AD.

Conflict of interest

The authors declare that they have no conflict of interest.

References

1. A. Melegaro, N. J. Gay, G. F. Medley, Estimating the transmission parameters of pneumococcal carriage in households, *Epidemiol Infect.*, **132** (2004), 433–441. <https://doi.org/10.1017/s0950268804001980>
2. E. Joseph, Mathematical analysis of prevention and control strategies of pneumonia in adults and children, University of Dar es Salaam, 2012.
3. D. Ssebuliba, Mathematical modelling of the effectiveness of two training interventions on infectious diseases in Uganda, PhD Thesis, Stellenbosch University, 2013.
4. J. Ong'ala, J. Y. T. Mugisha, P. Oleche, Mathematical model for Pneumonia dynamics with carriers, *Int. J. Math. Anal.*, **7** (2013), 2457–2473. <https://doi.org/10.12988/ijma.2013.35109>
5. H. W. Hethcote, The mathematics of infectious diseases, *SIAM Rev.*, **42** (2000), 599–653. <https://doi.org/10.1137/S0036144500371907>

6. G. T. Tilahun, O. D. Makinde, D. Malonza, Modelling and optimal control of pneumonia disease with cost-effective strategies, *J. Biol. Dynam.*, **11** (2017), 400–426. <https://doi.org/10.1080/17513758.2017.1337245>.
7. G. T. Tilahun, O. D. Makinde, D. Malonza, Co-dynamics of pneumonia and typhoid fever diseases with cost effective optimal control analysis, *Appl. Math. Comput.*, **316** (2018), 438–459. <https://doi.org/10.1016/j.amc.2017.07.063>
8. S. Saber, A. M. Alghamdi, G. A. Ahmed, K. M. Alshehri, Mathematical modelling and optimal control of pneumonia disease in sheep and goats in Al-Baha region with cost-effective strategies, *AIMS Mathematics*, **7** (2022), 12011–12049. <https://doi.org/10.3934/math.2022669>
9. I. Podlubny, *Fractional differential equations*, New York: Academic Press, 1999.
10. P. A. Naik, M. Yavuz, S. Qureshi, J. Zu, S. Townley, Modeling and analysis of COVID-19 epidemics with treatment in fractional derivatives using real data from Pakistan, *Eur. Phys. J. Plus*, **135** (2020), 795. <https://doi.org/10.1140/epjp/s13360-020-00819-5>
11. M. H. Alshehri, S. Saber, F. Z. Duraihem, Dynamical analysis of fractional-order of IVGTT glucose-insulin interaction, *Int. J. Nonlin. Sci. Num.*, **24** (2023), 1123–1140. <https://doi.org/10.1515/ijnsns-2020-0201>
12. M. H. Alshehri, F. Z. Duraihem, A. Alalyani, S. Saber, A Caputo (discretization) fractional-order model of glucose-insulin interaction: Numerical solution and comparisons with experimental data, *J. Taibah Univ. Sci.*, **15** (2021), 26–36. <https://doi.org/10.1080/16583655.2021.1872197>
13. S. Saber, A. Alalyani, Stability analysis and numerical simulations of IVGTT glucose-insulin interaction models with two time delays, *Math. Model. Anal.*, **27** (2022), 383–407. <https://doi.org/10.3846/mma.2022.14007>
14. A. Alalyani, S. Saber, Stability analysis and numerical simulations of the fractional COVID-19 pandemic model, *Int. J. Nonlin. Sci. Num.*, **24** (2023), 989–1002. <https://doi.org/10.1515/ijnsns-2021-0042>
15. N. Almutairi, S. Saber, Chaos control and numerical solution of time-varying fractional Newton-Leipnik system using fractional Atangana-Baleanu derivatives, *AIMS Mathematics*, **8** (2023), 25863–25887. <https://doi.org/10.3934/math.20231319>.
16. K. I. A. Ahmed, H. D. S. Adam, M. Y. Youssif, S. Saber, Different strategies for diabetes by mathematical modeling: modified minimal model, *Alex. Eng. J.*, **80** (2023), 74–87. <https://doi.org/10.1016/j.aej.2023.07.050>
17. K. I. A. Ahmed, H. D. S. Adam, M. Y. Youssif, S. Saber, Different strategies for diabetes by mathematical modeling: Applications of fractal-fractional derivatives in the sense of Atangana-Baleanu, *Results Phys.*, **2023** (2023), 106892. <https://doi.org/10.1016/j.rinp.2023.106892>
18. S. Saber, N. Almutairi, Chaos in a nonlinear Lorentz-Lü-Chen system via the fractal fractional operator of Atangana-Baleanu, submitted for publication.
19. D. Baleanu, B. Shiri, Generalized fractional differential equations for past dynamic, *AIMS Mathematics*, **7** (2022), 14394–14418. <https://doi.org/10.3934/math.2022793>

20. B. Shiri, G. C. Wu, D. Baleanu, Terminal value problems for the nonlinear systems of fractional differential equations, *Appl. Numer. Math.*, **170** (2021), 162–178. <https://doi.org/10.1016/j.apnum.2021.06.015>
21. B. Shiri, D. Baleanu, All linear fractional derivatives with power functions' convolution kernel and interpolation properties, *Chaos Soliton. Fract.*, **170** (2023), 113399. <https://doi.org/10.1016/j.chaos.2023.113399>.
22. C. Xu, D. Mu, Y. Pan, C. Aouiti, L. Yao, Exploring bifurcation in a fractional-order predator-prey system with mixed delays, *J. Appl. Anal. Comput.*, **13** (2023), 1119–1136. <https://doi.org/10.11948/20210313>
23. C. Xu, D. Mu, Z. Liu, Y. Pang, C. Aouitid, O. Tun, et al., Bifurcation dynamics and control mechanism of a fractional-order delayed Brusselator chemical reaction model, *Match Commun. Math. Co.*, **89** (2023), 73–106. <https://doi.org/10.46793/match.89-1.073X>
24. P. Li, Y. Lu, C. Xu, J. Ren, Insight into Hopf bifurcation and control methods in fractional order BAM neural networks incorporating symmetric structure and delay, *Cogn. Comput.*, **2023** (2023), 02. <https://doi.org/10.1007/s12559-023-10155-2>
25. P. Li, R. Gao, C. Xu, S. Ahmad, Y. Li, A. Akgul, Bifurcation behavior and PD^γ control mechanism of a fractional delayed genetic regulatory model. *Chaos Soliton. Fract.*, **168** (2023), 113219. <https://doi.org/10.1016/j.chaos.2023.113219>
26. P. A. Naik, Global dynamics of a fractional-order SIR epidemic model with memory, *Int. J. Biomath.*, **13** (2020), 2050071. <https://doi.org/10.1142/S1793524520500710>
27. M. B. Ghori, P. A. Naik, J. Zu, Z. Eskandari, M. Naik, Global dynamics and bifurcation analysis of a fractional-order SEIR epidemic model with saturation incidence rate, *Math. Method. Appl. Sci.*, **45** (2022), 3665–3688. <https://doi.org/10.1002/mma.8010>
28. A. Ahmad, M. Farman, P. A. Naik, N. Zafar, A. Akgul, M. U. Saleem, Modeling and numerical investigation of fractional-order bovine babesiosis disease, *Numer. Meth. Part. D. E.*, **37** (2021), 1946–1964. <https://doi.org/10.1002/num.22632>
29. M. Farman, A. Akgül, T. Abdeljawad, P. A. Naik, N. Bukhari, A. Ahmad, Modeling and analysis of fractional order Ebola virus model with Mittag-Leffler kernel, *Alex. Eng. J.*, **61** (2022), 2062–2073. <https://doi.org/10.1016/j.aej.2021.07.040>
30. P. A. Naik, K. M. Owolabi, M. Yavuz, J. Zu, Chaotic dynamics of a fractional order HIV-1 model involving AIDS-related cancer cells, *Chaos Soliton. Fract.*, **140** (2020), 110272. <https://doi.org/10.1016/j.chaos.2020.110272>
31. H. Khan, J. Gómez-Aguilar, A. Alkhazzan, A. Khan, A fractional order HIV-TB coinfection model with nonsingular Mittag-Leffler law, *Math. Method. Appl. Sci.*, **43** (2020), 3786–3806. <https://doi.org/10.1002/mma.6155>.
32. H. Khan, F. Jarad, T. Abdeljawad, A. Khan, A singular ABC-fractional differential equation with p-Laplacian operator, *Chaos Soliton. Fract.*, **129** (2019), 56–61. <https://doi.org/10.1016/j.chaos.2019.08.017>

33. A. Atangana, E. Alabaraoye, Solving a system of fractional partial differential equations arising in the model of HIV infection of CD4+ cells and attractor one-dimensional Keller-Segel equations, *Adv. Differ. Equ.*, **94** (2013), 94. <https://doi.org/10.1186/1687-1847-2013-94>
34. S. K. Choi, B. Kang, N. Koo, Stability for Caputo fractional differential systems, *Abstr. Appl. Anal.*, **2014** (2014), 631419. <https://doi.org/10.1155/2014/631419>
35. H. Li, L. Zhang, C. Hu, Y. Jiang, Z. Teng, Dynamical analysis of a fractional-order predator prey model incorporating a prey refuge, *J. Appl. Math. Comput.*, **54** (2016), 435–449. <https://doi.org/10.1007/s12190-016-1017-8>
36. A. Oname, M. Abbas, A. Abdel-Aty, Assessing the impact of SARS-CoV-2 infection on the dynamics of dengue and HIV via fractional derivatives, *Chaos Soliton. Fract.*, **162** (2022), 112427. <https://doi.org/10.1016/j.chaos.2022.112427>
37. D. Baleanu, A. Fernandez, A. Akgül, On a fractional operator combining proportional and classical differintegrals, *Mathematics*, **8** (2000), 360. <https://doi.org/10.3390/math8030360>
38. D. Baleanu, S. Arshad, A. Jajarmi, W. Shokat, F. A. Ghassabzade, M. Wali, Dynamical behaviours and stability analysis of a generalized fractional model with a real case study, *J. Adv. Res.*, **48** (2023), 157–173. <https://doi.org/10.1016/j.jare.2022.08.010>
39. H. Delvari, D. Baleanu, J. Sadati, Stability analysis of Caputo fractional-order non-linear systems revisited, *Nonlinear Dyn.*, **67** (2012), 2433–2439. <https://doi.org/10.1007/s11071-011-0157-5>
40. D. Baleanu, M. Hasanabadi, A. M. Vaziri, A. Jajarmi, A new intervention strategy for an HIV/AIDS transmission by a general fractional modeling and an optimal control approach, *Chaos Soliton. Fract.*, **167** (2023), 113078. <https://doi.org/10.1016/j.chaos.2022.113078>
41. A. Akgul, A novel method for a fractional derivative with non-local and nonsingular kernel, *Chaos Soliton. Fract.*, **114** (2018), 478–482. <https://doi.org/10.1016/j.chaos.2018.07.032>
42. A. Akgul, M. Modanli, Crank-Nicholson difference method and reproducing kernel function for third order fractional differential equations in the sense of Atangana-Baleanu Caputo derivative, *Chaos Soliton. Fract.*, **127** (2019), 10–16. <https://doi.org/10.1016/j.chaos.2019.06.011>
43. M. Caputo, M. Fabrizio, A new definition of fractional derivative without singular kernel, *Progr. Fract. Differ. Appl.*, **1** (2015), 73–85. <https://doi.org/10.12785/pfda/010201>
44. M. Toufik, A. Atangana, New numerical approximation of fractional derivative with non-local and non-singular kernel: Application to chaotic models, *Eur. Phys. J. Plus*, **132** (2017), 444. <https://doi.org/10.1140/epjp/i2017-11717-0>
45. S. A. Jose, R. Ramachandran, D. Baleanu, H. S. Panigoro, J. Alzabut, V. E. Balas, Computational dynamics of a fractional order substance addictions transfer model with Atangana-Baleanu-Caputo derivative, *Math. Method. Appl. Sci.*, **46** (2023), 5060–5085. <https://doi.org/10.1002/mma.8818>
46. A. Atangana, On the new fractional derivative and application to nonlinear Fisher's reaction-diffusion equation, *Appl. Math. Comput.*, **273** (2016), 948–956. <https://doi.org/10.1016/j.amc.2015.10.021>
47. M. Caputo, Linear model of dissipation whose Q is almost frequency independent-II, *Geophys. J. Int.*, **13** (1967), 529–539. <https://doi.org/10.1111/j.1365-246X.1967.tb02303.x>

48. S. K. Choi, B. Kang, N. Koo, Stability for Caputo fractional differential systems, *Abstr. Appl. Anal.*, **2014** (2014), 631419. <https://doi.org/10.1155/2014/631419>
49. P. van den Driessche, J. Watmough, Reproduction numbers and subthreshold endemic equilibria for compartmental models of disease transmission, *Math. Biosci.*, **180** (2002), 29–48. [https://doi.org/10.1016/S0025-5564\(02\)00108-6](https://doi.org/10.1016/S0025-5564(02)00108-6)
50. S. Baba, O. D. Makinde, Optimal control of HIV/AIDS in the workplace in the presence of careless individuals, *Comput. Math. Method. M.*, **2014** (2014), 831506. <https://doi.org/10.1155/2014/831506>
51. S. Uçar, E. Uçar, N. Özdemir, Z. Hammouch, Mathematical analysis and numerical simulation for a smoking model with Atangana-Baleanu derivative, *Chaos Soliton. Fract.*, **118** (2019), 300–306, <https://doi.org/10.1016/j.chaos.2018.12.003>
52. M. Al-Refai, K. Pal, New aspects of Caputo-Fabrizio fractional derivative, *Progr. Fract. Differ. Appl.*, **5** (2019), 157–166. <https://doi.org/10.18576/pfda/050206>
53. A. Atangana, D. Baleanu, New fractional derivatives with nonlocal and non-singular kernel: Theory and application to heat transfer model, *Therm. Sci.*, **20** (2016), 763–769.
54. A. Atangana, S. Qureshi, Modeling attractors of chaotic dynamical systems with fractal-fractional operators, *Chao Soliton. Fract.*, **123** (2019), 320–337, <https://doi.org/10.1016/j.chaos.2019.04.020>
55. S. Uçar, Analysis of hepatitis B disease with fractal-fractional Caputo derivative using real data from Turkey, *J. Comput. Appl. Math.*, **419** (2023), 114692, <https://doi.org/10.1016/j.cam.2022.114692>
56. I. Koca, Modeling the heat flow equation with fractional-fractal differentiation, *Chaos Soliton. Fract.*, **128** (2019), 83–91. <https://doi.org/10.1016/j.chaos.2019.07.014>
57. Z. Ali, F. Rabiei, K. Shah, T. Khodadadi, Fractal-fractional order dynamical behavior of an HIV/AIDS epidemic mathematical model, *Eur. Phys. J. Plus*, **136** (2021), 36. <https://doi.org/10.1140/epjp/s13360-020-00994-5>
58. L. Zhang, M. ur Rahman, H. Qu, M. Arfan, Adnan, Fractal-fractional Anthroponotic Cutaneous Leishmania model study in sense of Caputo derivative, *Alex. Eng. J.*, **61** (2022), 4423–4433, <https://doi.org/10.1016/j.aej.2021.10.001>
59. H. Khan, K. Alam, H. Gulzar, S. Etemad, S. Rezapour, A case study of fractal-fractional tuberculosis model in China: Existence and stability theories along with numerical simulations, *Math. Comput. Simulat.*, **198** (2022), 455–473. <https://doi.org/10.1016/j.matcom.2022.03.009>
60. J. K. K. Asamoah, Fractal-fractional model and numerical scheme based on Newton polynomial for Q fever disease under Atangana Baleanu derivative, *Results Phys.*, **34** (2022), 105189. <https://doi.org/10.1016/j.rinp.2022.105189>
61. K. M. Saad, M. Alqhtani, J. F. Gomez-Aguilar, Fractal-fractional study of the hepatitis C virus infection model, *Results Phys.*, **19** (2020), 103555. <https://doi.org/10.1016/j.rinp.2020.103555>
62. S. Etemad, I. Avci, P. Kumar, D. Baleanu, S. Rezapour, Some novel mathematical analysis on the fractal-fractional model of the AH1N1/09 virus and its generalized Caputo-type version, *Chaos Soliton. Fract.*, **162** (2020), 112511. <https://doi.org/10.1016/j.chaos.2022.112511>

63. H. Khan, J. Alzabut, A. Shah, S. Etemad, S. Rezapour, C. Park, A study on the fractal-fractional tobacco smoking model, *AIMS Mathematics*, **7** (2022), 13887–13909. <https://doi.org/10.3934/math.2022767>
64. H. Najafi, S. Etemad, N. Patanarapeelert, J. K. K. Asamoah, S. Rezapour, T. Sitthiwirattam, A study on dynamics of CD4+ T-cells under the effect of HIV-1 infection based on a mathematical fractal-fractional model via the Adams-Bashforth scheme and Newton polynomials, *Mathematics*, **10** (2022), 1366. <https://doi.org/10.3390/math10091366>
65. S. Etemad, I. Avci, P. Kumar, D. Baleanu, S. Rezapour, Some novel mathematical analysis on the fractal-fractional model of the AH1N1/09 virus and its generalized Caputo-type version, *Chaos Soliton. Fract.*, **162** (2022), 112511. <https://doi.org/10.1016/j.chaos.2022.112511>
66. A. Atangana, Fractal-fractional differentiation and integration: connecting fractal calculus and fractional calculus to predict complex system, *Chaos Soliton. Fract.*, **102** (2017), 396–406. <https://doi.org/10.1016/j.chaos.2017.04.027>
67. H. Khan, F. Ahmad, O. Tunç, M. Idrees, On fractal-fractional Covid-19 mathematical model, *Chaos Soliton. Fract.*, **157** (2022), 111937. <https://doi.org/10.1016/j.chaos.2022.111937> .
68. K. A. Abro, A. Atangana, Numerical and mathematical analysis of induction motor by means of AB-fractal-fractional differentiation actuated by drilling system, *Numer. Methods Partial Differential Eq.*, **38** (2022), 293–307. <https://doi.org/10.1002/num.22618>
69. K. M. Owolabi, A. Atangana, A. Akgul, Modelling and analysis of fractal-fractional partial differential equations: application to reaction-diffusion model, *Alex. Eng. J.*, **59** (2020), 2477–2490. <https://doi.org/10.1016/j.aej.2020.03.022>
70. A. Atangana, A. Akgul, K. M. Owolabi, Analysis of fractal fractional differential equations, *Alex. Eng. J.*, **59** (2020), 1117–1134. <https://api.semanticscholar.org/CorpusID:212831086>
71. K. M. Owolabi, A. Shikongo, A. Atangana, Fractal fractional derivative operator method on MCF-7 cell line dynamics, In: *Methods of mathematical modelling and computation for complex systems*, Cham: Springer, 2022, 319–339. <https://doi.org/10.1016/j.aej.2021.10.001>
72. S. Qureshi, A. Atangana, Fractal-fractional differentiation for the modeling and mathematical analysis of nonlinear diarrhea transmission dynamics under the use of real data, *Chaos Soliton. Fract.*, **136** (2020), 109812. <https://doi.org/10.1016/j.chaos.2020.109812>
73. K. Shah, M. Arfan, I. Mahariq, A. Ahmadian, S. Salahshour, M. Ferrara, Fractal-fractional mathematical model addressing the situation of Corona virus in Pakistan, *Results Phys.*, **19** (2020), 103560. <https://doi.org/10.1016/j.rinp.2020.103560>
74. K. I. A. Ahmed, H. D. S. Adam, M. Y. Youssif, S. Saber, Different strategies for diabetes by mathematical modeling: modified minimal model, *Alex. Eng. J.*, **80** (2023), 74–87. <https://doi.org/10.1016/j.aej.2023.07.050>
75. K. I. A. Ahmed, H. D. S. Adam, M. Y. Youssif, S. Saber, Different strategies for diabetes by mathematical modeling: Applications of fractal-fractional derivatives in the sense of Atangana-Baleanu, *Results Phys.*, **2023** (2023), 106892. <https://doi.org/10.1016/j.rinp.2023.106892>

76. A. Atangana, Fractal-fractional differentiation and integration: Connecting fractal calculus and fractional calculus to predict complex system, *Chaos Soliton. Fract.*, **102** (2017), 396–406. <https://doi.org/10.1016/j.chaos.2017.04.027>
77. K. A. Abro, A. Atangana, A comparative study of convective fluid motion in rotating cavity via Atangana-Baleanu and Caputo-Fabrizio fractal-fractional differentiations, *Eur. Phys. J. Plus*, **135** (2020), 226. <https://doi.org/10.1140/epjp/s13360-020-00136-x>
78. P. Li, L. Han, C. Xu, X. Peng, M. ur Rahman, S. Shi, Dynamical properties of a meminductor chaotic system with fractal-fractional power law operator, *Chaos Soliton. Fract.*, **175** (2023), 114040. <https://doi.org/10.1016/j.chaos.2023.114040>
79. A. Jamal, A. Ullah, S. Ahmad, S. Sarwar, A. Shokri, A survey of (2+1)-dimensional KdV-mKdV equation using nonlocal Caputo fractal-fractional operator, *Results Phys.*, **46** (2023), 106294. <https://doi.org/10.1016/j.rinp.2023.106294>
80. S. M. Ulam, *A collection of mathematical problems*, New York: Interscience, 1960.
81. S. M. Ulam, *Problems in modern mathematics*, London: Dover Publications, 2004.
82. Z. M. Odibat, N. T. Shawagfeh, Generalized Taylor's formula, *Appl. Math. Comput.*, **186** (2007), 286–293. <https://doi.org/10.1016/j.amc.2006.07.102>
83. Z. M. Odibat, S. M. Momani, An algorithm for the numerical solution of differential equations of fractional order, *J. Appl. Math. Informatics*, **26** (2008), 15–27.



AIMS Press

© 2023 the Author(s), licensee AIMS Press. This is an open access article distributed under the terms of the Creative Commons Attribution License (<http://creativecommons.org/licenses/by/4.0>)